Article



# Coordination Polymers With the Pyrazine-2,5-Diyldimethanol Linker – Supramolecular Networks Through Robust Hydrogen and Halogen Bonds

Mahsa Armaghan *, Tobias Stürzer , Christoph Janiak *

Posted Date: 31 May 2023

doi: 10.20944/preprints202305.2265.v1

Keywords: Pyrazine-diyldimethanol; coordination polymers; hydrogen bonding interaction; halogen bonding interaction

*Article*

# Coordination Polymers with the Pyrazine-2,5-Diyldimethanol Linker—Supramolecular Networks through Robust Hydrogen and Halogen Bonds

**Mahsa Armaghan [1,*] Tobias Stürzer [2] and Christoph Janiak [1,*]**

[1] Institut für Anorganische Chemie und Strukturchemie, Heinrich-Heine Universität Düsseldorf, 40204 Düsseldorf, Germany; armaghan@uni-duesseldorf.de; janiak@uni-duesseldorf.de

[2] Bruker AXS GmbH Östliche Rheinbrückenstraße 49 76187 Karlsruhe Germany; Tobias.Stuerzer@bruker.com

* Correspondence: armaghan@uni-duesseldorf.de (M.A.) ; janiak@uni-duesseldorf.de (C.J.) ; Tel.: +49 211 81-13669

**Abstract:** The synthesis and crystal structure of pyrazine-2,5-diyldimethanol (**pzydmH2**, $C_8H_8N_2O_2$) a new symmetric water-soluble N,O-chelating tetra-dentate organic ligand is reported and an environmentally friendly method was used to synthesize coordination compounds in water under ambient conditions from the reaction of **pzydmH2** with the halide salts of Cu(II), Zn(II), Hg(II) and Cd(II): {[Cu(**pzydmH2**)$_{0.5}$(μ-Br)(Br)($H_2O$)]·$H_2O$}$_n$ **1**, {[$Zn_2$(**pzydmH2**)(μ-Cl)$_3$($H_2O$)]·$H_2O$}$_n$ **2**, [$Hg_2$(**pzydmH2**)$_{0.5}$(μ-Cl)$_2$$(Cl)_2$]$_n$ **3**, {[$Cd_2$(**pzydmH2**)(μ-Cl)$_4$]·$H_2O$}$_n$ **4**, and {[$Cd_2$(**pzydmH2**)(μ-Br)$_4$]·$H_2O$}$_n$ **5**. Single-crystal X-ray diffraction analysis revealed that **1**-**3** are 1D coordination polymers and **4** and **5** are 3D coordination networks, all constructed by bridging pyrazine-2,5-diyldimethanol and halogen ions. The hydroxyl groups in the organic linker extend the 1D chains to non-covalent 3D networks. In all non-covalent and covalent 3D networks water molecules were trapped by strong hydrogen bond interactions. Supramolecular analysis revealed strong O-H···O, O-H···N, O-H···X and week of C-H···O, C-H···X (X = Cl, Br) hydrogen bonds, as well as π-π(pyrazine ring), metal-halogen···π(pyrazine ring) and O-H···ring(5-membered chelate ring) interactions. Also X···O weak halogen bonds are present in **1**-**5** (X = Cl and Br).

**Keywords:** Pyrazine-diyldimethanol; coordination polymers; hydrogen bonding interaction; halogen bonding interaction.

## 1. Introduction

Pyridine–alcohol based ligands are versatile N,O chelating organic linkers because of the rich σ donating and strong coordination toward a wide range of transition metal ions. The large number of structures directed us in earlier toward designing and synthesizing new polydentate mixed-functional ligands providing hydroxyl group beside the nitrogen atom and a carboxylic acid group in a different position of the pyridine ring [1–3]. Our studies on 2-hydroxylmethylpyridine-carboxylate ligands (Scheme 1) showed that in mononuclear complexes, the pyridine alcohol group has a higher tendency for coordination to the first row transition metal ions than the carboxylate group [4–]. Therefore, we planned to extend our studies on pyrazine alcohols by synthesizing pyrazine-2,5-diyldimethanol (**pzydmH2**) (Scheme 1) as a new organic linker and probably a large diversity of stable coordination compounds. Scheme 2 depicts the potential variety of **pzydmH2** coordination modes to create different coordination geometries [8–10]. Despite being able to coordinate to the transition metal ions, **pzydmH2** can interact in several different ways, for example, both nitrogen atoms and the hydroxyl groups can involve in hydrogen bonds. The pyrazine C−H can act as weak hydrogen bond donor, and also pyrazine ring can involve in various π-interactions [11–14]. Furthermore, considering that a pyrazine ring and alcohol groups can be part of biological systems, coordination compounds assembled from pyrazine-diyldimethanol based ligands with biocompatible or non-biocompatible metals can be biologically important [15–17]. Moreover,

Preprints (www.preprints.org) | NOT PEER-REVIEWED | Posted: 31 May 2023 doi:10.20944/preprints202305.2265.v1



**pzdmH2** is a symmetric water-soluble organic ligand and the high solubility of pyrazine alcohol based ligands is important for their roles in biochemistry.

This research work first focused on the synthesis of pyrazine-2,5-diyldimethanol (**pzdmH2**, $C_8H_8N_2O_2$) and then the synthesis of coordination compounds assembled from **pzdmH2** and the first row and d10 transition metal elements by using metal halide salts as inorganic precursors [18,19]. The high water solubility of **pzydmH2** and the water soluble metal halide salts $CuBr_2$, $ZnCl_2$, $HgCl_2$, $CdCl_2{\cdot}H_2O$ and $CdBr_2{\cdot}4H_2O$ allowed us to study the coordination modes of **pyzmH2** to Cu(II), Zn(II), Hg(II) and Cd(II) without using organic solvents, high temperature or pressure. We hope that this approach will facilitate the synthesis of water stable, and cost-effective coordination compounds that can be easily scaled up in water.

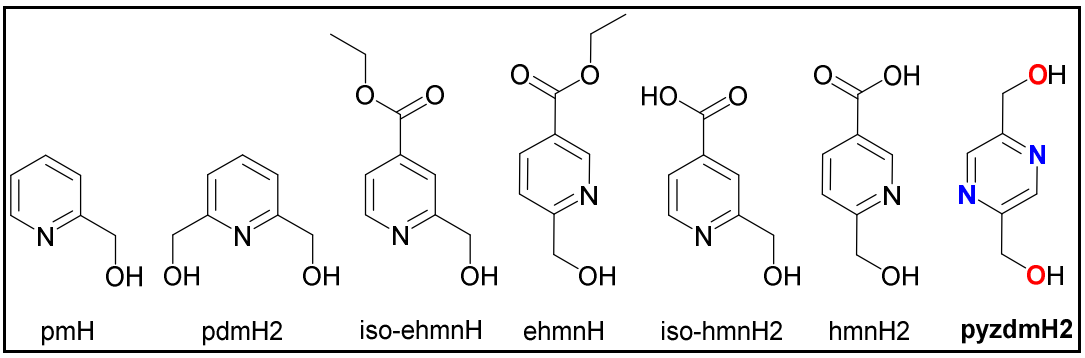


**Scheme 1.** Pyridine-alcohol based ligands and pyrazine-2,5-diyldimethanol (**pzdmH2**).

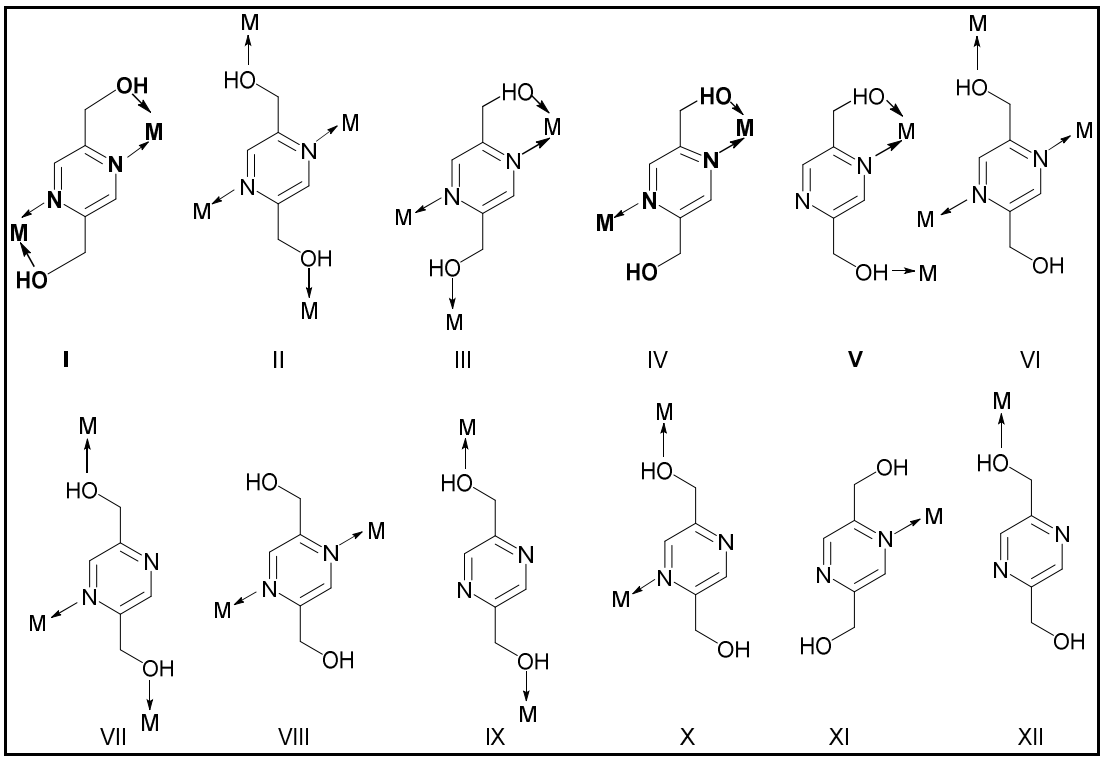


**Scheme 2.** The possible coordination modes of pyrazine-2,5-diyldimethanol. **I** and **IV** have been observed in compounds **1-5**.

## 2. Materials and Methods

Reagents were obtained from commercial sources and used without further purification. $^1$H NMR and $^{13}$C NMR spectra were recorded on a Bruker Avancse III-300. IR spectra were recorded on a Bruker Tensor 37 IR spectrometer equipped with an ATR unit (Platinum ATR-QL, Diamond).

 doi:10.20944/preprints202305.2265.v1



Elemental analyses were conducted with a PerkinElmer CHN 2400 Analyzer. The powder X-ray diffraction patterns (PXRD) were obtained on a Bruker D2 Phaser powder diffractometer with a flat silicon, low background sample holder, at 30 kV, 10 mA for Cu-K$\alpha$ radiation ($\lambda$ = 1.5418 Å).

*2.1. Single X-ray crystallography*

Suitable crystals were carefully selected under a polarizing microscope, covered in protective oil and mounted on a cryo-loop. The single crystal X-ray diffraction measurements of **pzydmH2** and **1-5** were carried out on a Bruker Kappa APEX-II CCD diffractometer with Mo-K$\alpha$ radiation (microfocus tube, multi-layer mirror system, $\lambda$ = 0.71073 Å) applying $\phi$- and $\omega$-scans at temperatures 140(2) and 296(2) K [20]. Evaluation of the crystal system, orientation matrix, and cell dimensions were carried out with the APEX4 software suite [21–24]. SMART, SAINT, and SADABS [25,26] were used for the calculations of data collection/unit cell refinement, frame integration/data reduction and multi-scan absorption correction, respectively. XPREP (Sheldrick, 2008) was used to set up files for structure solutions. The structures were solved straightforwardly by direct methods (SHELX-97, XS and XT) and refine on F2 by full-matrix least-squares techniques with the SHELXTL and OLEX2-1.3 programs [27–29]. All non-hydrogen atoms in **pzydmH2** and **1-5** were refined anisotropically. All hydrogen atoms in **pzydmH2** and **1-5** were seen in the related Fourier maps after all non-hydrogen atoms were located. However, to achieve better data over parameter, H-atoms connected to $C_{aromatic}$ and $C_{aliphatic}$ were fixed at calculated positions riding model approximation on the atoms, AFIX 43 and AFIX 23 respectively ($C_{aromatic}$—H 0.930, and $C_{aliphatic}$—H 0.970 Å the values for room temperate, and $C_{aromatic}$—H 0.950 $C_{aliphatic}$—H 0.990, Å the values for 140 K) with U(H) set to 1.2U(C). All the hydrogen atom positions of the hydroxyl groups of **pzydmH2** and coordinated and non-coordinated water molecules were assigned by difference Fourier calculations with SHELXLE-2017 and OLEX2-1.3 [29,30] and then refined with U(H) set to 1.5U(O). The detailed structural refinement including the applied restrained and constrained for **pzydmH2** and **1-5** were given in the supplementary information. The crystallographic data and structural refinement results along with further details of data collections and analyses are listed in Table S1 (Supporting Information). Molecular Graphics were drawn with 3D visualized software Diamond and Mercury [31–34].

*2.2. Synthetic procedures for pzydmH2*

2.2.1. Preparation of dimethyl pyrazine-2,5-dicarboxylate (a)

Synthesizing dimethyl pyrazine-2,5-dicarboxylate is in two steps (Scheme 3) [2,3]. the first step is the oxidation of 2,5-dimethylpyrazine (9.9 g, 91.70 mmol) using selenium dioxide (49.50 g, 446.10 mmol) by reflux in a 10:1 pyridine/water mixture overnight. The hot mixture is filtered to remove the bulk of the elemental selenium produced and then evaporated to dryness. The crude pyrazine-2,5-dicarboxylic acid is then esterified using thionylchloride (7.02 g, 58.98 mmol) in methanol by refluxing overnight. Dimethylpyrazine-2,5-dicarboxylate (**a**) is isolated as analytically pure crystals in 40% yield from 2,5-dimethylpyrazine by slow evaporation from methanol. Collected as an orange solid, the yield was ~ (5 g, 40%). Melting Point 164 °C, Selected IR data ($cm^{-1}$), (KBr pellet): 3424 (m), 3076 (s), 3016 (w), 2960 (m), 2853 (w), 1720 (vs), 1541 (w), 1472 (m), 1433 (s), 1359 (s), 1278 (vs), 1202 (w), 1182 (m), 1143 (s), 1019 (s), 958 (m), 822 (m), 757 (s), 679 (w), 493 (w), 465 (m), 424 (m) $cm^{-1}$. MS (EI, 80 °C, m/z): 196 [M]. Anal. calcd (solvent-free): (%) for $C_8H_8N_2O_4$ (169.16 g/mol): C 48.98, H 4.11, N 14.28; found: C 48.31, H 4.54, N 14.97 %. $^1$H NMR (300 MHz, $CDCl_3$) δ: 9.33 (s, 2H, pzyH), 4.22 (s, 6H, $CH_3$) ppm (Figure S1). $^{13}$C {1H} NMR (75 MHz, $CDCl_3$) δ: 163.5 (pzyCO), 145.5 (pzyH), 145.3 (pzyH), 53.5 ($OCH_3$) ppm (Figure S2).

Preprints (www.preprints.org) | NOT PEER-REVIEWED | Posted: 31 May 2023 doi:10.20944/preprints202305.2265.v1



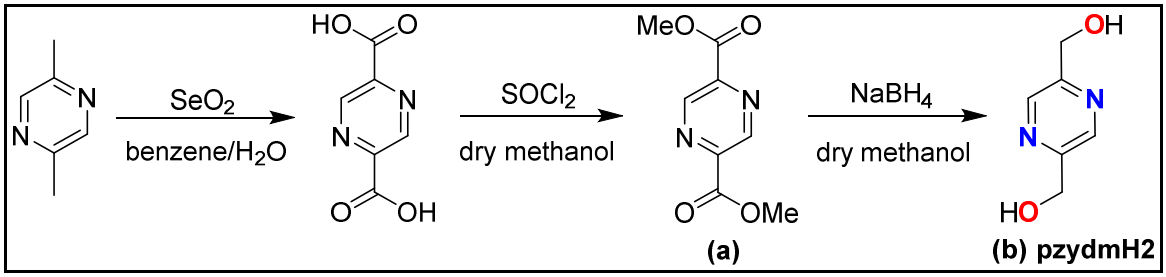


**Scheme 3.** Synthesis of pzydmH2.

2.2.2. Preparation of pyrazine-2,5-diyldimethanol (b)

To a yellowish methanol solution (50 mL) containing dimethyl pyrazine-2,5-dicarboxylate (2.0 g, 10.2 mmol), $NaBH_4$ (3.1 g, 81.95 mmol) was slowly added at 0 °C with stirring under inter atmosphere. After the addition was completed, the mixture was stirred for 3 h at the room temperature overnight. The reaction was quenched by dropwise addition of $H_2O$. The resulting dark precipitate was filtered off, followed by solvent evaporation. Continues liquid-liquid extraction of the resulting mixture with $CHCl_3$ and $H_2O$ for two days, followed by solvent evaporation gave colorless single crystal of pyrazine-2,5-diyldimethanol (0.5 g, 35%). The long extraction is necessary as the pyrazine-2,5-diyldimethanol formed is very soluble in water. The obtained crystals of **pzydmH2** was stored in the mother liquor until single crystal analysis. Melting Point 77-80 °C, Selected IR data ($cm^{-1}$), (KBr pellet): 3320 (b), 2920(w), 2832 (w), 1490 (m), 1444 (s), 1351 (s), 1286 (m), 1220 (w), 1153 (m), 1063 (vs), 1022 (s), 911 (w), 873 (w), 783 (w), 732 (m), 669 (m), 604 (m), 529 (w), 451 (w). MS (EI, 60 °C): 140 m/z: 140 [M], 139 [M-H]. Anal. calcd (solvent-free): (%) for $C_6H_8N_2O_2$ (140.14 g/mol): C 51.42, H 5.75, N 19.99; found: C 51.49, H 5.52, N 19.51. $^1$H NMR (300 MHz, Acetone-$d_6$) δ: 8.51 (s, 2H, pzyH), 4.64 (s, OH), 4.62 (s, 4H, CH2), 4.50 (t, J 2 Hz, OH) ppm (Figure S3). $^{13}$C {1H} NMR (101 MHz, Acetone-$d_6$): d 155.8 (pzyCH2), 142.1 (pzy), 64.0 (CH2) ppm (Figure S4).

*2.3. Syntheses of 1-5.*

Water solutions of $CuBr_2$ (2.67 mg, 0.048 mmol), $ZnCl_2$ (9.81 mg, 0.072 mmol), $HgCl_2$ (19.37 mg, 0.072 mmol), $CdCl_2{\cdot}H_2O$ (4.36 mg, 0.024 mmol), $CdBr_2{\cdot}4H_2O$ (8.18 mg, 0.024 mmol), and pyrazine-2,5-diyldimethanol (3.33 mg, 0.024 mmol) were mixed in $H_2O$ (3 mL) in glass tubes to give greenish, colorless, colorless, colorless and yellowish solutions respectively. The solutions place on the top of the water in an ultrasonic bath overnight at room temperature. The block-shaped crystals of **1-5** were obtained by slow evaporation of water over several weeks at room temperature. The obtained crystals were stored in the mother liquor until single crystal analysis.

## 3. Result and discussion

*3.1. Synthesis organic linker and coordination polymers*

To explore and understanding of the diverse coordination modes of **pzdmH2** to Cu(II), Zn(II), Hg(II) and Cd(II) and their role on the crystal structure design, herein we describe the crystal structure of **pzdmH2** and **1-5**. The coordination modes **I** and **IV** in scheme 2 have been observed in **1-5**. In this research work, the most conventional non-covalent interactions (NCIs), hydrogen bond, π-π stacking, and halogen bond interactions as the main stabilizing forces in supramolecular structure and maybe 3D covalent network formation have been widely investigated [35–37]. Furthermore, other secondary bonding interactions (SBIs), like oxygen...oxygen interaction which may also play a considerable role in supramolecular interactions or crystal structure design have been surveyed [38–41].

Based upon the previous successful synthesis of a serious of functionalized 2-hydroxymethyl pyridine carboxylate esters or carboxylic acids [2,3], **pzydmH2** has been synthesized in three steps (Scheme 3). The oxidation of 2,5-dimethylpyrazine by selenium dioxide followed by the esterification

Preprints (www.preprints.org) | NOT PEER-REVIEWED | Posted: 31 May 2023 doi:10.20944/preprints202305.2265.v1



and then the reduction of dimethyl pyrazine-2,5-dicarboxylate. The pure product, **pzydmH2,** was obtained after purification by crystallization.

By using aqueous solutions of $CuBr_2$, $ZnCl_2$, $HgCl_2$, $CdCl_2{\cdot}H_2O$ and $CdBr_2{\cdot}4H_2O$ with aqueous solution of **pzdmH2** under ambient conditions in ultrasonic bath, five new coordination polymers **1-5** were synthesized and isolated in the single-crystal solid phase. The molar ratio of $CuBr_2$, $ZnCl_2$, $HgCl_2$, $CdCl_2{\cdot}H_2O$ and $CdBr_2{\cdot}4H_2O$ to **pzydmH2** was kept at 1:2, 1:3, 1:3, 1:1 and 1:1 for preparing **1-5** respectively. Single crystals of compounds **1-5** were grown in aqueous solution. The compounds $\{[Cu(pzydmH2)_{0.5}(\mu\text{-}Br)(Br)(H_2O)]\cdot H_2O\}_n$ **1**, $\{[Zn_2(pzydmH2)(\mu\text{-}Cl)(Cl)_3(H_2O)]\cdot H_2O\}_n$ **2**, $[Hg_2(pzydmH2)_{0.5}(\mu\text{-}Cl)_2(Cl)_2]_n$ **3**, $\{[Cd_2(pzydmH2)(\mu\text{-}Cl)_4]\cdot H_2O\}_n$ **4**, and $\{[Cd_2(pzydmH2)(\mu\text{-}Br)_4]\cdot H_2O\}_n$ **5** were derived from single-crystal X-ray structure analyses. **1-3** feature 1D polymeric structures constructed from $\mu_2$-halide, $\mu_2$-**pzydmH2** and double $\mu_2$-halide (Scheme 4). $Cd^{2+}$ compounds **4** and **5** feature 3D network structures also constructed from double $\mu_2$-halide and $\mu_2$-**pzydmH2** (Scheme 5). In all compounds, except for **3**, **pzydmH2** functions as a tetra-dentate linker that forms two chelate rings (model **I** in Scheme 2). However, in **3**, one of the hydroxyl groups of **pzydmH2** functions as a side arm, resulting in a tri-dentate linker (model **IV** in Scheme 2). We observed that water molecules and the hydroxyl groups from **pzydmH2** have key roles in the formation of the 3D non-covalent and covalent networks of compounds **1-5**, due to the strong hydrogen bond interactions present within these structures. The key hydrogen bond interactions are listed in Table 1.

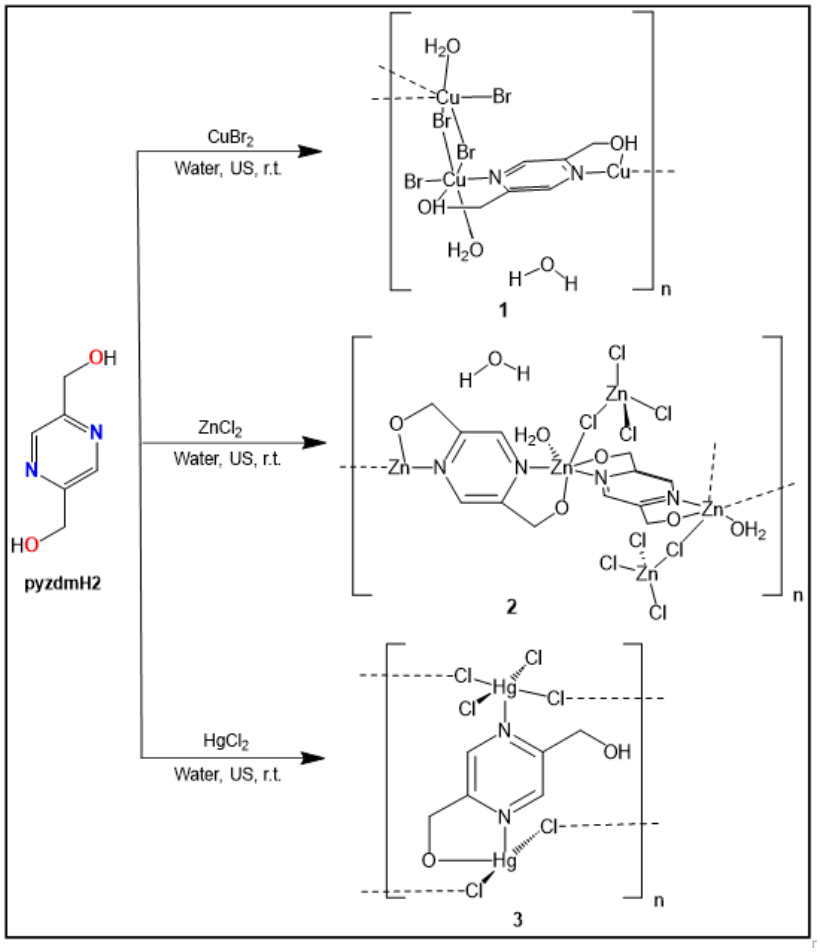


**Scheme 4.** Schematic presentation of the synthesis of **1-3**.

Preprints (www.preprints.org) | NOT PEER-REVIEWED | Posted: 31 May 2023 doi:10.20944/preprints202305.2265.v1



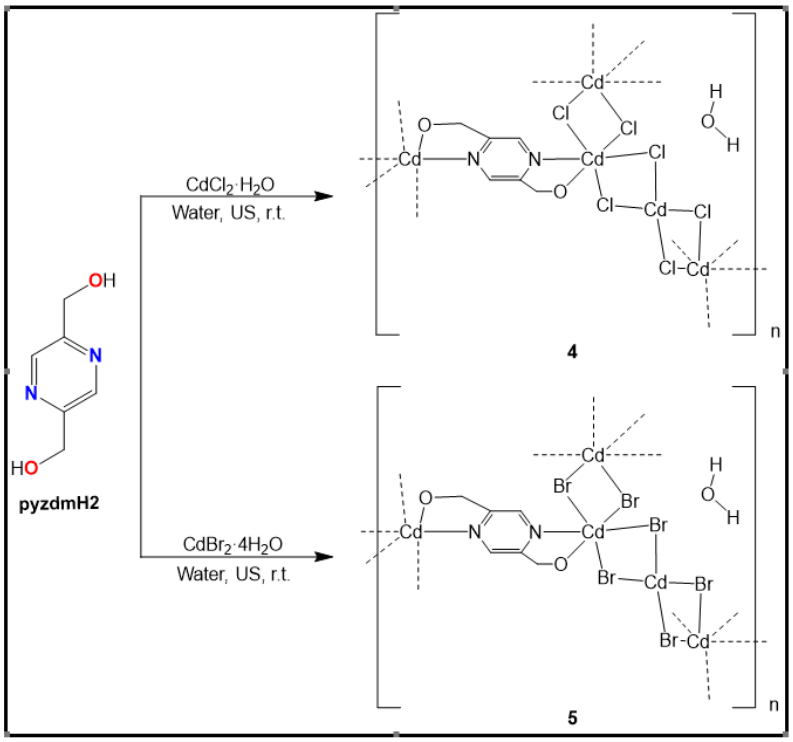


**Scheme 5.** Schematic presentation of the synthesis of **4** and **5**.

**Table 1.** Key hydrogen bond interactions for **pzydmH2** and **1-5** [Å and °] with standard uncertainties in parentheses.

| D-H···A | d(D-H) | d(H···A) | d(D···A) | <(DHA) |
|---|---|---|---|---|
| **pzydmH2** | | | | |
| O(1)-H(1)···N(2) | 0.87(16) | **1.97(16)** | **2.84(12)** | 171 |
| O(2)-H(2)···O(3)#iii | 0.85(16) | **1.87(16)** | **2.72(11)** | 174 |
| O(3)-H(3)···N(3)#ii | 0.85(16) | **1.99(16)** | **2.80(11)** | 159 |
| Symmetry transformations used to generate equivalent atoms: ii = -x+2, -y+2, -z+1 #iii = x, -y+3/2, z-1/2. | | | | |
| **1** | | | | |
| O(1)-H(1)···O(2)#iii | 0.82(16) | **1.82(2)** | **2.63(18)** | 172 |
| O(2)-H(2A)···O(3)#iv | 0.82(2) | **1.96(2)** | **2.77(21)** | 173 |
| O(2)-H(2B)···O(3)#iii | 0.78(2) | **2.06(2)** | **2.83(20)** | 169 |
| O(3)-H(3A)···Br(1)#v | 0.87(2) | 2.55(2) | 3.23(16) | 135 |
| O(3)-H(3B)···Br(2)#vi | 0.80(2) | 2.49(2) | 3.29(15) | 178 |
| Symmetry transformations used to generate equivalent atoms: iii = 1-x, 1-y, 1-z, iv = 1-x, -1/2+y, 1/2-z, v = 1-x, -1/2+y, 1/2-z, vi = 1-x, 1-y, -z. | | | | |
| **2** | | | | |
| O(1)-H(1)···O(4)#iii | 0.87(2) | **1.72(2)** | **2.59(3)** | **175** |
| O(2)-H(2)···Cl(2)#iv | 0.83(3) | 2.25(3) | 3.08(19) | **176** |
| O(3)-H(3B)···Cl(3)#iv | 0.82(4) | 2.38(4) | 3.16(2) | 160 |

| | | | | |
|---|---|---|---|---|
| O(3)-H(3A)···Cl(4)#v | 0.82(4) | 2.29(4) | 3.10(2) | 170 |
| O(4)-H(4A)···Cl(4) | 0.85(3) | 2.38(3) | 3.16(2) | 153 |
| O(4)-H(4B)···Cl(2) | 0.84(3) | 2.55(4) | 3.29(2) | 148 |

Symmetry transformations used to generate equivalent atoms: iii = x-1, y, z, iv = x-1/2, -y+3/2, z+1/2, v = -x+1/2, y+1/2, -z+1/2.

| **3** | | | | |
|---|---|---|---|---|
| *Intra* O(1)-H(1)···O(2)#i | 0.82(19) | **1.93(2)** | **2.73(3)** | 165 |
| *Intra* O(1)-H(1)···Cl(4)#i | 0.82(19) | 2.75(2) | 3.12(3) | 109 |
| O(2)-H(2)···O(1)#iii | 0.83(19) | 2.25(3) | 2.96(3) | 143 |
| O(2)-H(2)···Cl(2)#iii | 0.83(19) | 2.82(4) | 3.45(3) | 136 |

Symmetry transformations used to generate equivalent atoms: i = -x+2, -y+1, -z+1, iii = x, y, z-1.

| **4** | | | | |
|---|---|---|---|---|
| O(1)-H(1A)···O(2)#x | 0.85(6) | **1.83(10)** | **2.62(10)** | 154 |
| O(1)-H(1A)···O(2)#iv | 0.85(6) | **1.99(10)** | **2.69(10)** | 138 |
| O(1)-H(1B)···O(1)#iv | 0.85(8) | **1.82(10)** | **2.62(5)** | 156 |
| O(2)-H(2B)···O(1)#iv | 0.93 | **1.85** | **2.69(10)** | 149 |
| O(2)-H(2A)···Cl(2)#ii | 0.80 | 2.65(13) | 3.26(9) | 134 |
| O(2)-H(2A)···Cl(2)#v | 0.80 | 2.68(13) | 3.18(9) | 122 |

Symmetry transformations used to generate equivalent atoms: ii = -x+1,-y+1,-z+1, iv = -x+1,-y,-z+1, v = x, 1-y, 1/2+z, x = x, -y, z-1/2.

| **5** | | | | |
|---|---|---|---|---|
| O(1)-H(1A)#vi···O(2) | 0.85(6) | **1.83(7)** | **2.68(10)** | 172(8) |
| O(1)-H(1B)#v···O(1)#ii | 0.85(6) | **1.81(9)** | **2.64(5)** | 165(12) |
| O(2)-H(2B)···O(1)#v | 0.72 | **1.99** | **2.70(10)** | 165 |
| O(2)-H(2A)···Br(2) | 0.84 | 2.78 | 3.39(9) | 131 |
| O(2)-H(2A)···Br(2)#i | 0.84 | 2.88 | 3.33(9) | 115 |

Symmetry transformations used to generate equivalent atoms: i = -x+1, y, -z+3/2, ii = -x+1, -y+1, -z+1, v = x, y+1, z, vi = 1-x, y+1, 3/2-z,.

The hydrogen bond lengths highlighted in bold and used to indicate hydrogen bonds correspond to a bond that is typically between 0.45 and 0.20 Å shorter than the sum of the van der Waals radii of the atoms participating in the hydrogen bond. The bond angle that is highlighted in bold indicates angle that are close to 180 °.

3.1.1. Crystal structure of pyrazine-2,5-diyldimethanol (pzydmH2)

Pyrazine-2,5-diyldimethanol (**pzydmH2**) crystallizes in the monoclinic centrosymmetric $P2_1/c$ space group (Table S1). The atoms of one and a half formula unit in general positions define the asymmetric unit of the crystal structure in **pzydmH2** (Z = 6, Z' = 1.5). Figure 1 shows the atomic

Preprints (www.preprints.org) | NOT PEER-REVIEWED | Posted: 31 May 2023 doi:10.20944/preprints202305.2265.v1



displacement ellipsoids for the asymmetric unit and the atomic numbering in this compound. As shown in the Figure, one molecule is located on a crystallographic inversion center. Selected bond lengths, angles, and torsion angles are summarized in Table S2. **PzydmH2** crystallizes in two different conformations with regard to the dangling methanol groups ($H_2C$-OH). The methanol groups O1-H1, O2-H2 and O3-H3 are not coplanar with the attached pyrazine rings in the both conformations and are twisted with respect to the mean plane of the pyrazine rings by 135.14(1), 147.86(1), and 95.00(2)° respectively and ∠O1-H1-C1-C2, ∠O1$^{i}$-H1$^{i}$-C1$^{i}$-C2$^{i}$, ∠O2-H2-C4-C5, ∠O3-H3-C9-C8 torsion angles are 134.8, -134.8, 155.3, 78.8° respectively (see Table S2 for symmetry codes). In the crystal structure, the molecules pack in a one-dimensional strand-like arrangement generated by **pzydmH2** molecules of the same conformation (N2-C5-C6-N3-C8-C7) along the crystallographic *c*-axis. The adjacent **pzydmH2** molecules are connected in a side-by-side arrangement along the crystallographic *c*-axis through a strong hydrogen bond O2-H2···O3$^{iii}$ to generate the one-dimensional strands with intermolecular separation **1.87(16)** Å. These strands are sewn to the neighboring strands through the hydrogen bonds O3-H3···N3$^{ii}$ with intermolecular separation **1.99(16)** Å and are further sewn by aid of **pzydmH2** molecules, containing the pyrazine ring which is generated by a crystallographic inversion center, through a hydrogen bond O1-H1···N2 with intermolecular separation **1.97(16)** Å (Figure 2a). Apparently, these strong hydrogen bonds may play key role in directing the configuration of **pzydmH2** in the single crystal structure (Table 1). **PzydmH2** molecules from the same conformations are further stacked through hydrogen bonds C1-H1A···O1$^{v}$, C4-H4B···O2$^{iv}$ and C9-H9A···O3$^{v}$ (Figure 2b, Table S3) in such a manner that there are no strong π-π interaction between pyrazine rings (centroid···centroid distance 4.06 Å, Figure S5a, Table S4) [42]. One view of the crystal packing is depicted in Figure S5b.

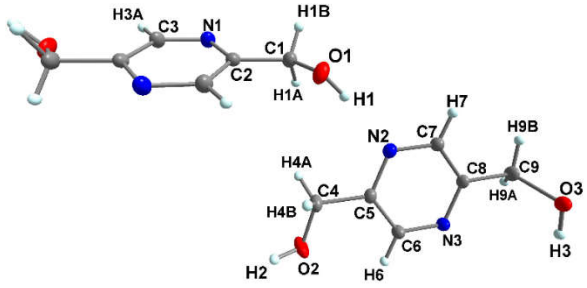


**Figure 1.** Expanded asymmetric unit of **pzydmH2** along with the atom labelling scheme. For the sake of clarity, hydrogen bonds are omitted. Displacement ellipsoid are drawn at the 50% probability level and H atoms are of arbitrary radii. Unlabeled atoms are generated by the symmetry operation i = 1–x, 1–y, –z.

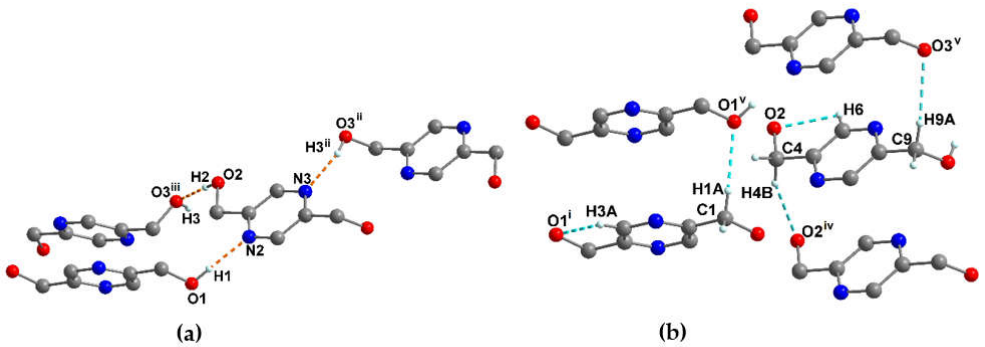


**Figure 2. (a)** Hydrogen bonds of the O-H···O, and the O-H···N types are depicted by dashed bonds in orange color. **(b)** Hydrogen bonds of the C-H···O type is depicted by dashed bonds in turquoise blue

color. Symmetry codes: i = 1-x, 1-y, -z #ii = -x+2, -y+2, -z+1 #iii = x, -y+3/2, z-1/2 #iv = x, -1+y, z #v = x,1+y, z.

3.1.2. Crystal structure of {[Cu(pzydmH2)$_{0.5}$(μ-Br)(Br)(H$_2$O)]·H$_2$O}$_n$ (1)

Compound **1** crystallizes in the monoclinic centrosymmetric space group *P*2$_1$/*c* (Table S1). It is a 1D-neutral coordination polymer in which the Cu$^{2+}$ ion is six-coordinated. The asymmetric unit of the polymeric structure contains one copper ion (Cu$^{2+}$), half of **pzydmH2** which forms a bridging tetra-dentate linker, two bromine ions which are coordinated to the copper ion as terminal (Br2) and bridging (Br1) ligands, a coordinated water molecule (aqua ligand) (O2H2AH2B) and a non-coordinated water molecule (O3H3AH3B) and all atoms are in general positions (Z = 4, Z' = 1). The 2+ charge on Cu is balanced by the bridging and terminal bromine ions. Figure 3 shows the atomic displacement ellipsoids for the asymmetric unit, along with the atomic numbering in **1**. The Cu$^{2+}$ ion in the polymeric structure **1** is surrounded by the N and O atoms from **pyzdmH2** in a chelating configuration, which are bonded in a relatively short distance from the central Cu$^{2+}$ ion [Cu-O1 = 1.9968(12), Cu-N1 = 2.0281(13) Å], two symmetry-related bridging bromine atoms in a *cis*-configuration [Cu-Br1 = 2.4112(3), and Cu-Br1$^{ii}$ = 3.0672(3) Å], one terminal bromine atom [Cu-Br2 = 2.3627(3) Å], and finally, an O atom from the coordinated water molecule [Cu-O = 2.6590(15) Å]. This coordination environment forms a Jahn-Teller distorted tetragonal geometry around the d$^9$ Cu$^{2+}$ ion. The chelating N and O atoms from **pzydmH2**, the terminal bromine atom (Br2) *trans* to the N atom and one of the bridging Br atoms (Br1) trans to the O atom fill the equatorial plane. The axial positions are occupied by the coordinated water molecule and the symmetry-related bridging bromine atom to Br1. The five-membered chelate ring, Cg(2) = Cu-O1-C1-C2-N1, with the bite distance of 2.587 Å deviates with the angle O1-Cu-N1 from 90° by about 10° and subsequently the angles ∠N1-Cu-Br1, ∠Br1-Cu-Br2 and ∠O1-Cu-Br2 deviate by about 6.4°, 5.3° and 2°, respectively [43]. Selected bond distances, angles and torsion angles of **1** are summarized in Table S2.

Each Cu$^{2+}$ center connects to two adjacent Cu$^{2+}$ centers through a pair of the bridging bromine atoms (Cu…Cu 3.99(4) Å) and through the tetra-dentate bridging **pzydmH2** linker (Cu…Cu 6.80(4) Å) to generate a one-dimensional stair-like chain structure which extends along the crystallographic *c*-axis (Figure 4a). At the center of the four-membered Br1-Cu-Br1$^{ii}$-Cu$^{ii}$ lies a crystallographic inversion center which renders this ring planar by symmetry, (∠Cu-Br1$^{ii}$-Cu$^{ii}$ = 92.78(9)°). Adjacent chains are connected by strong hydrogen bonds between the OH groups of **pzydmH2** in one chain and O atoms from the coordinated water molecules in the neighboring symmetry-related chain [O1-H1···O2$^{iii}$ = **1.82(2)** Å] to form a supramolecular 2D sheet which extends within the *ac* plane (Figure 4b, see Table S2 for symmetry codes). The coordinated water molecule connects to two symmetry-related crystal water molecules through two strong hydrogen bonds O2-H2A···O3$^{iv}$, and O2-H2B···O3$^{iii}$. Furthermore, the non-coordinated water molecule is involved in two hydrogen bonds O3-H3A···Br1$^{v}$ and O3-H3B···Br2$^{vi}$ (Figure 4c, Table 1). The last four hydrogen bonds link the adjacent 2D sheets to extend a 3D non-covalent network along the *b*-axis (Figure 5a). The one-dimensional chains and 2D sheets are further linked through longer hydrogen and halogen bond interactions listed in the Table S5 and S7. In addition, there are a short inter-chain interactions of O-H···ring(5-membered chelate ring) (Table S6) [44]. There are no π-π(pyrazine ring) interactions in the crystal structure of **1**. Figure 5b shows the crystal-packing diagram of **1** with the unit cell.

Preprints (www.preprints.org) | NOT PEER-REVIEWED | Posted: 31 May 2023 doi:10.20944/preprints202305.2265.v1



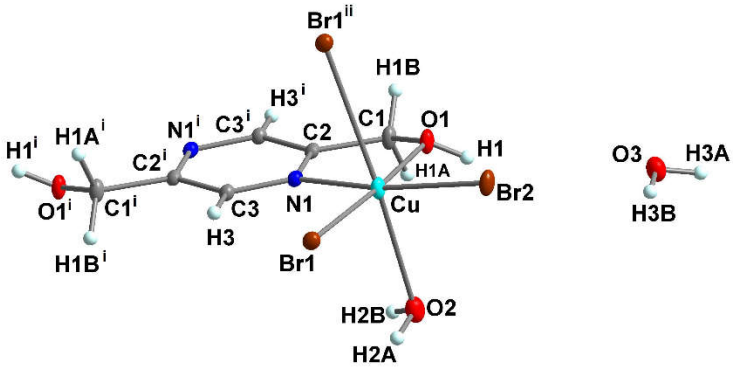


**Figure 3.** Asymmetric unit of **1** with the full coordination environment around $Cu^{2+}$ along with the atom labelling scheme, the atoms defining the asymmetric unit are indicated without symmetry codes, showing displacement ellipsoids at the 50% probability level, H atoms are of arbitrary radii. Symmetry codes: i = 2-x,1-y,2-z, and ii = 2-x,1-y,1-z.

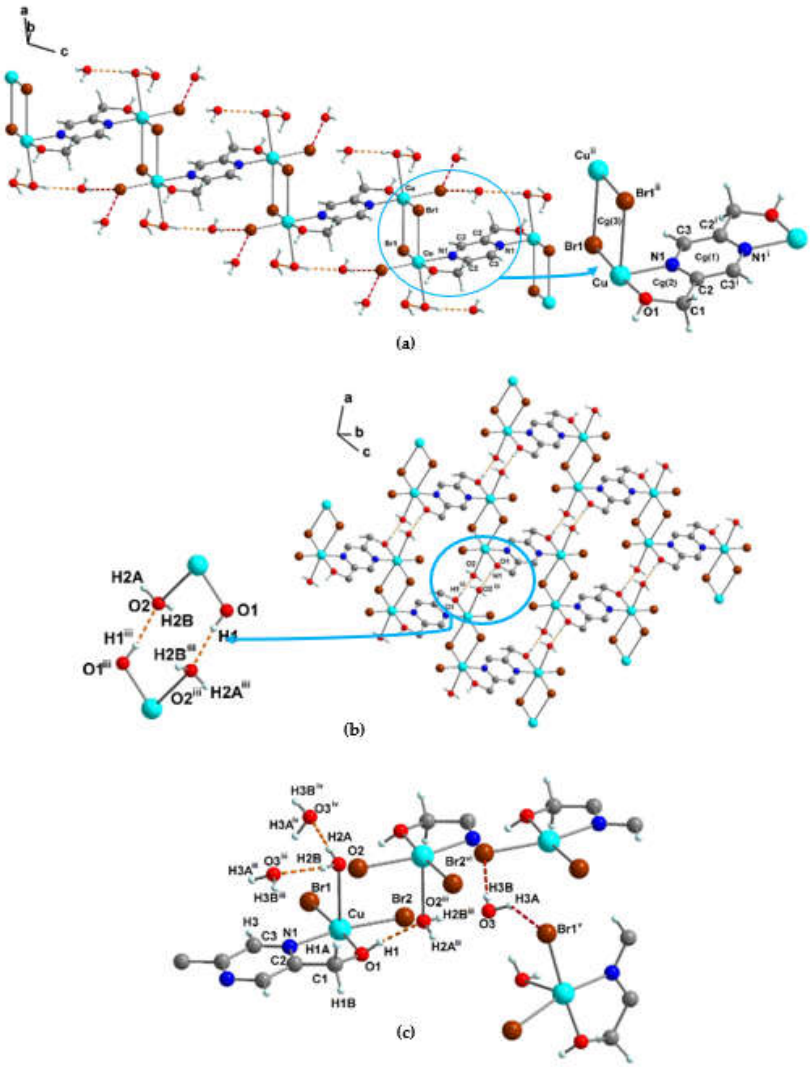


**Figure 4. (a)** One-dimensional stair-like chain in the structure of 1 along with the magnified depiction of Cg(1), Cg(2) and Cg(3). **(b)** A view of the 2D sheet created by the O1-H1···O2 hydrogen bond in the ac plane, depicted by dashed bonds in orange color. For the sake of clarity, only the hydrogens of the coordinated water molecule and the hydroxyl group from pzydmH2 are shown. **(c)** Hydrogen bonds O-H···O, and O-H···Br are depicted by dashed bonds in orange and lateritious colors, respectively.

Preprints (www.preprints.org) | NOT PEER-REVIEWED | Posted: 31 May 2023 doi:10.20944/preprints202305.2265.v1



Symmetry codes: i = 2-x, 1-y, 2-z, ii = 2-x, 1-y, 1-z, iii = 1-x, 1-y, 1-z, iv = 1-x, -1/2+y, 1/2-z, v = 1-x, 1/2+y, 1/2-z, vi = 1-x, 1-y, -z.

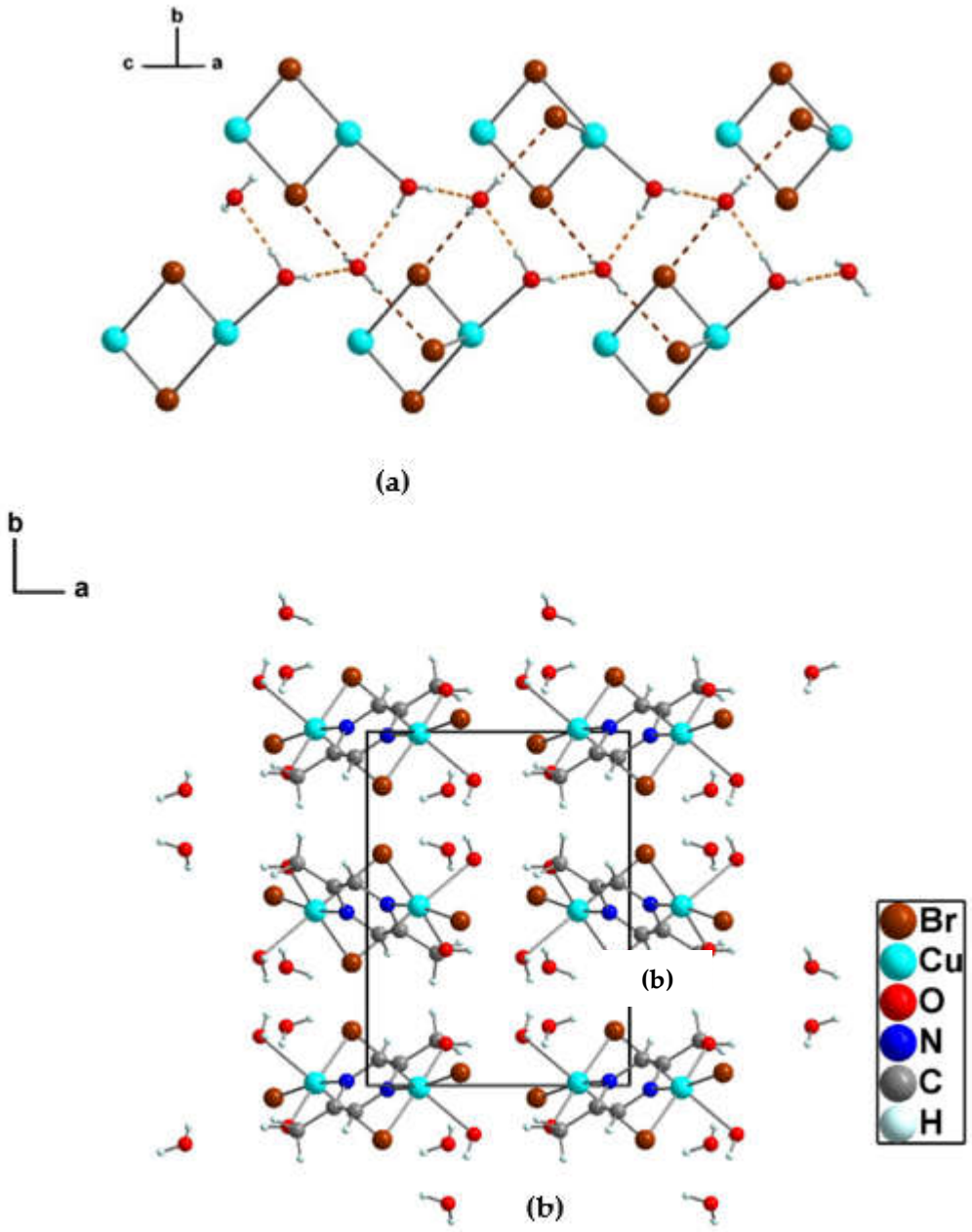


**Figure 5. (a)** Hydrogen bond network between the non-covalent 2D-sheets along the *b*-axis, **(b)** Cell packing diagram of 1 viewed along the *c*-axis with the color codes.

3.1.3. Crystal structure of $\{[Zn_2(pzydmH2)(\mu\text{-}Cl)(Cl)_3(H_2O)]\cdot H_2O\}_n$ (2)

Compound **2** crystallizes in the centrosymmetric monoclinic space group $P2_1/n$ (Table S1) as a 1D-neutral coordination polymer. The asymmetric unit contains two independent zinc ions (Zn1 and Zn2), one bridging tetra-dentate **pzydmH2** linker between two symmetry-related zinc ions (Zn1, $Zn1^{i}$), one bridging chloride ion (Cl1) which coordinates to two independent zinc ions (Zn1 and Zn2), three terminal chloride ions (Cl2, Cl3, Cl4) coordinated to Zn2, a coordinated water molecule (O3H3BH3A) and a non-coordinated crystal water molecule (O4H4AH4B), and all atoms are in

Preprints (www.preprints.org) | NOT PEER-REVIEWED | Posted: 31 May 2023 doi:10.20944/preprints202305.2265.v1



general positions (Z = 4, Z' = 1). Figure 6a shows the atomic displacement ellipsoids for the asymmetric unit in **2**, along with the atomic numbering.

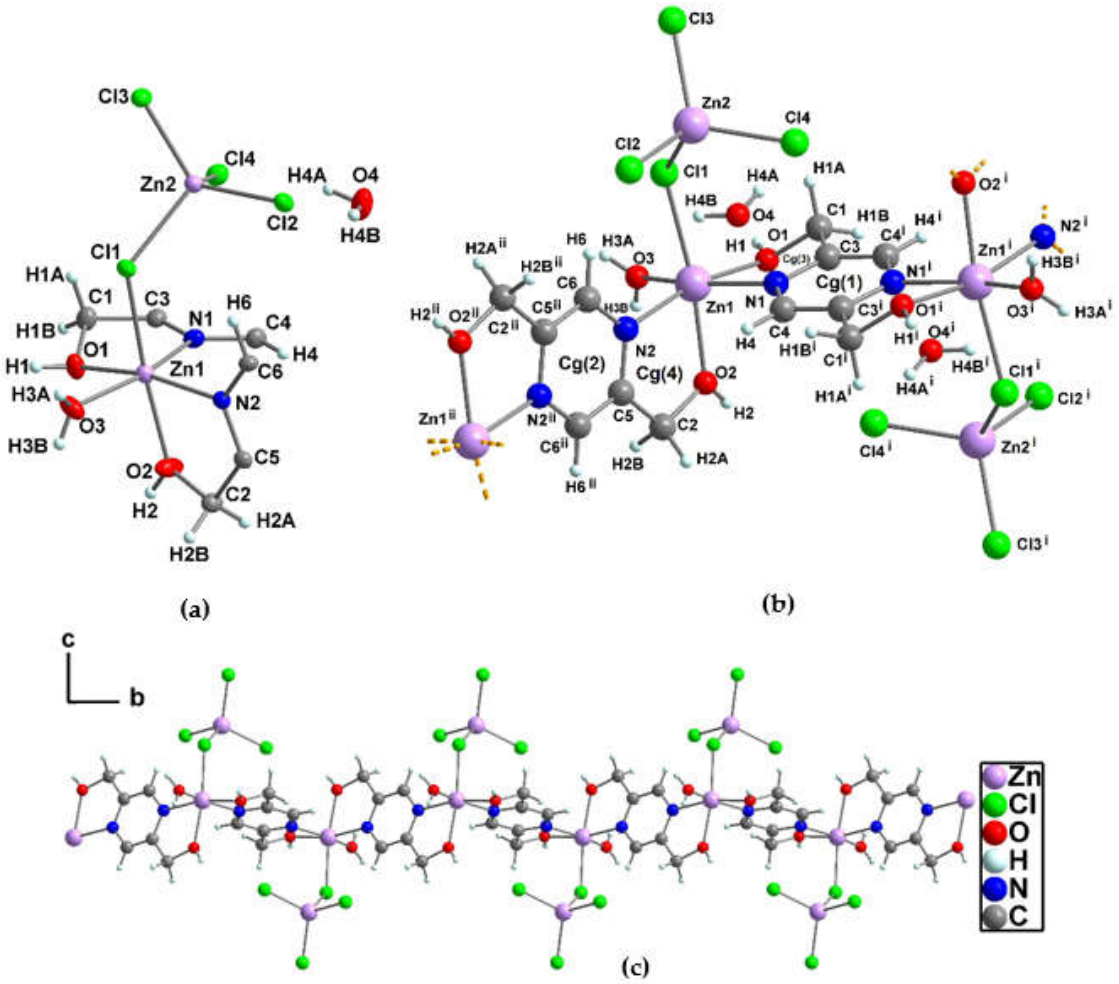


**Figure 6. (a)** Asymmetric unit of **2** along with the atom labelling scheme, showing displacement ellipsoids at the 50% probability level, H atoms are of arbitrary radii, for the sake of clarity, hydrogen bonds are omitted. **(b)** Ball and stick presentation of the spatial full coordination environment around Zn1 and Zn2 in **2**. **(c)** One-dimensional polymeric zig-zag chain structure in **2** along the *b* axis with color codes. Symmetry codes: i = 1-x, 1-y, 1-z, ii = 1-x, 2-y, 1-z. Cg(1) = N1-C3-C4$^{i}$-N1$^{i}$-C3$^{i}$–C4, Cg(2) = N2-C5-C6$^{ii}$-N2$^{ii}$-C5$^{ii}$–C6), Cg(3) = Zn1-O1-C1-C3-N1, Cg(4) = Zn1-O2-C2-C5-N2.

The structure of **2** contains two kinds of coordination geometries around the $Zn^{2+}$ ions, a six-coordinated Zn1 in a distorted octahedral geometry and a four-coordinated Zn2 in a close to tetrahedral geometry (Zn2) (Figure 6b). The distorted octahedral Zn1 is defined by two chelating **pzydmH2** [Zn1-O1 = 2.0972(17), Zn1-N1 = 2.112(2), Zn1-O2 = 2.1259(18), Zn1-N2 = 2.1451(19) Å], an O atom from the coordinated water molecule [Zn1-O3 = 2.0447(18) Å] and the bridging chlorine (Cl1) from the tetrachloridozincate complex $[Zn(2)Cl_4]^{2-}$ [Zn1-Cl1 = 2.4669(6) Å]. It should also be notable that the nitrogen atoms from the two **pzydmH2** chelators (N1, N2) are in *trans*-configuration position to O atoms from the aqua ligand (O3) and an O (O1) from **pzdmH2**, respectively which all occupy the equatorial positions. The axial positions are filled by the chlorine from the tetrachloridozincate complex and an O atom from **pzydmH2** (O2) [O(2)-Zn(1)-Cl(1) = 171.37(5)°]. The two **pyzdmH2** ligands are in two slightly different conformations regarding the methanol groups. The methanol group O1-H1 attached to the pyrazine ring Cg(1) has the torsion angle ∠O(1)-C(1)-C(3)-N(1) = -26.5(3)°, and the methanol group O2-H2 attached to the pyrazine ring Cg(2) has the torsion angle ∠O(2)-C(2)-C(5)-N(2) = 6.9(3)°. The tetrahedral coordination geometry of $Zn^{2+}$ is determined by four

Preprints (www.preprints.org) | NOT PEER-REVIEWED | Posted: 31 May 2023 doi:10.20944/preprints202305.2265.v1



chloride ions that are coordinated in both bridging and terminal modes. [Zn2-Cl1 = 2.3115(6), Zn2-Cl2 = 2.2773(6), Zn2-Cl3 = 2.2529(6), Zn2-Cl4 = 2.2531(6) Å]. Table S2 summarizes the bond lengths, bond and torsion angles that have been selected for the compound **2**.

The symmetry-related adjacent octahedral zinc centers are bridged by the two **pyzdmH2** linkers to create a 1D zig-zag chain along the *b* crystallography axis (Figure 6c). In compound **2**, strong intra-chain hydrogen bond interactions were identified, including *intra* O1-H1···O3 = 2.68(3), O3-H3B···O2 = 2.88(4), C6-H6···Cl2 = 2.77(4), C6-H6···Cl1 = 2.86(4) Å. In addition, halogen···π(pyrazine ring) and O-H···ring(chelate ring) interactions are observed, including *intra* Cl4···Cg(1) = 3.2821(11), *intra* O3-H3B···Cg(4) = 3.00(4) Å. These interactions likely along with the constraint imposed by the chelation on the N1–Zn1–O1 and N2–Zn1–O2 angles contribute to the distortion of the octahedral geometry around Zn1. The five-membered chelate rings, Cg(3) = Zn1-O1-C1-C3-N1, Cg(4) = Zn1-O2-C2-C5-N2, have a bite distance of 2.578 and 2.598 Å and an angle ∠O1-Zn1-N1 and ∠O2-Zn1-N2 75.53(7) and 74.94(7)°, respectively (Figure 7a, b, and c see Table S8 and S9) [43]. Adjacent one-dimensional zig-zag chains in **2** are connected in a side-to-side manner by the crystal water molecules through three inter-chain hydrogen bonds, resulting in the construction of a 2D sheet that extends within the *ab* plane. The hydrogen bonds were created between the crystal water molecule and the OH group of **pyzdmH2** and the chloride atoms from the tetrachloridozincate complex [O1-H1···O4$^{iii}$ , O4-H4A···Cl4, and O4-H4B···Cl2], (see Table 1 and Table S8). It should be highlighted that a brief O···O distance is present in the hydrogen bond interaction between O1-H1 and O4$^{iii}$, with the distance and angle measuring 2.59(3) Å and 174.74°, respectively for O1···O4$^{iii}$, ∠O1-H1···O4$^{iii}$ [45] (Table S10). Stacking of these sheets along the *c* direction through the hydrogen bond types of O-H···Cl, C-H···O and C-H···Cl with distances between 2.25-3.03 Å yields a 3D supramolecular structure in which the crystal water molecules have been trapped. The hydrogen bond interactions as well as the halogen bond interactions which are depicted in Figure 7d and listed in Table S8 and S10, respectively, contribute in the stacking. Figure 8a and b illustrate the one-dimensional polymeric zig-zag chain structure as well as the supramolecular structure containing crystal water molecules in **2**.

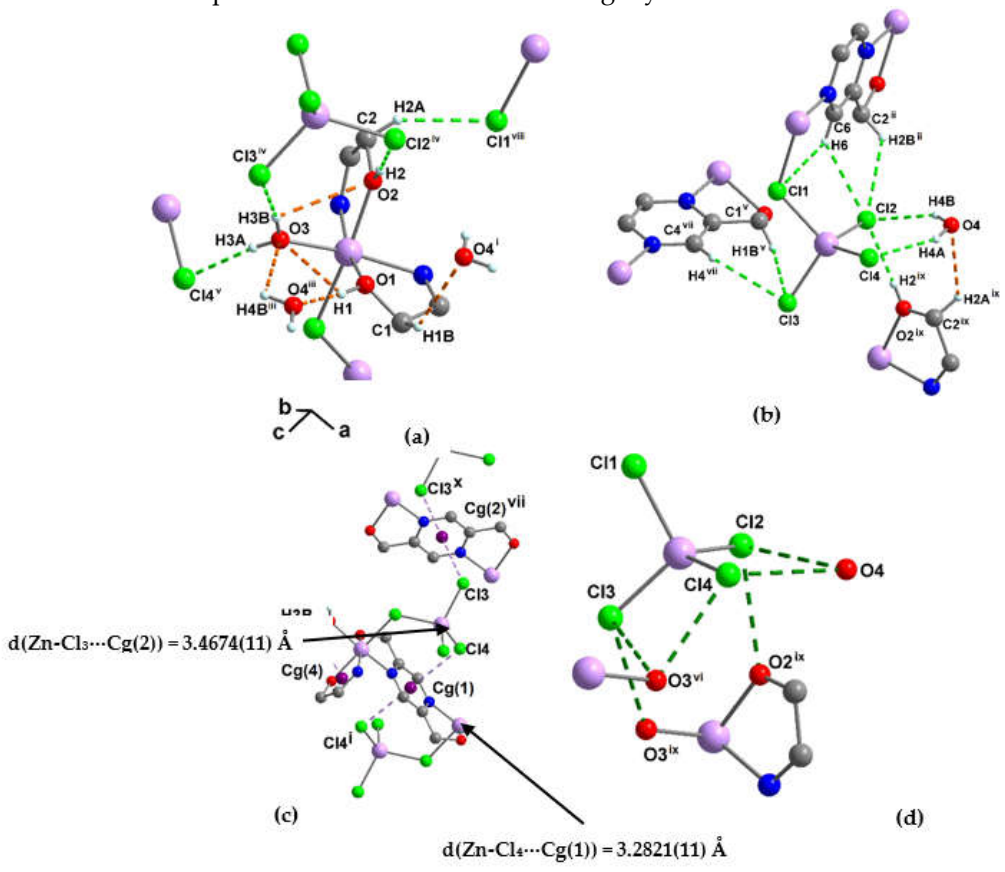


**Figure 7. (a, b)** Hydrogen bond types of O-H···O, O-H···Cl, C-H···O, and C-H···Cl in the structure of **2**, depicted by dashed bonds in orange, light green, orange, light green colors, respectively. **(c)** Halogen

Preprints (www.preprints.org) | NOT PEER-REVIEWED | Posted: 31 May 2023 doi:10.20944/preprints202305.2265.v1



bond type of Cl···π(pyrazine) and O-H···ring(5-membered chelate ring) interaction are depicted by dashed bonds in light purple color. **(d)** Halogen bond interaction O···Cl is depicted by dashed bonds in dark green color. For clarity, only the atoms involved in the short interactions are shown. Symmetry codes: i = 1-x, 1-y, 1-z, ii = 1-x, 2-y, 1-z, iii = x-1, y, z, iv = x-1/2, -y+3/2, z+1/2, v = -x+1/2, y+1/2, -z+1/2, vi = -x+1/2, y-1/2, -z+1/2, vii = x-1/2, -y+3/2, z-1/2, viii = x+1/2, -y+3/2, z+1/2, ix = x+1/2, -y+3/2, z-1/2, x = -x, 1-y, -z. Cg(1) = N1- C3-C4#i-N1#i-C3#i –C4, Cg(2) = N2- C5-C6#ii-N2#ii-C5#ii –C6, Cg(3) = Zn1-O1-C1-C3-N1, Cg(4) = Zn1-O2-C2-C5-N2.

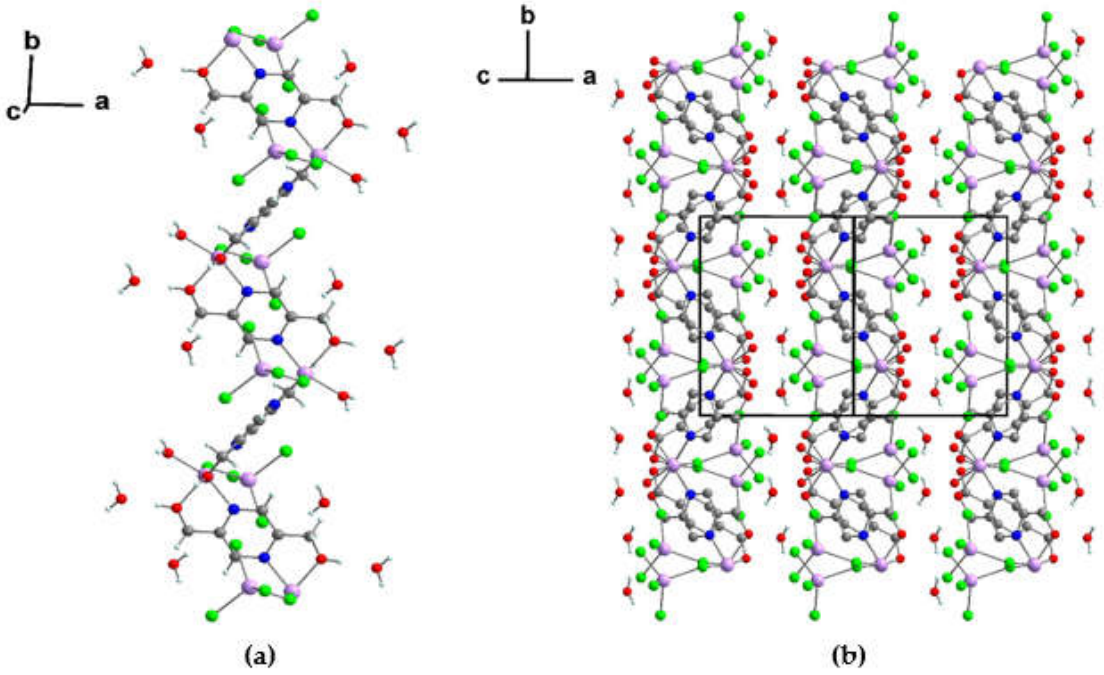


**Figure 8. (a)** One-dimensional polymeric zig-zag chain structure with crystal water molecules in **2** along the *b* axis. **(b)** Stacking of the 2D sheets within the *ab* plane in **2**.

3.1.4. Crystal structure of $[Hg_2(pzydmH2)(\mu\text{-}Cl)_2(Cl)_2]_n$ (3)

In the triclinic system, compound **3** crystallizes in the centrosymmetric space group *P*-1 (refer to Table S1) as a 1D-neutral coordination polymer. The polymeric crystal structure's asymmetric unit contains, two independent mercury $Hg^{2+}$ ions (Hg1 and Hg2), one **pzydmH2** as an organic linker which forms an unilaterally tridentate chelate linker between the two mercury ions Hg1 and Hg2 with one hanging uncoordinated OH group (O2-H2), two chloride ions are acting as bridges in a fashion that connects the Hg1 and Hg2 ions (Cl1, Cl2), and two chloride ions which are terminally coordinated to Hg2 ion (Cl3, Cl4), all atoms are in general positions (Z = 2, Z' = 1). The overall positive charge of the two $Hg^{2+}$ cations was neutralized by the four chloride ions in each formula unit in **3**. In Figure 9, the asymmetric unit of **3** is depicted, which displays two distinct coordination geometries around the $Hg^{2+}$ ions. Specifically, Hg1 exhibits a four-coordinated see-saw-like geometry, while Hg2 displays a five-coordinated square pyramid geometry, as illustrated in Figures 9b and 9c. The Hg1 cation is chelated by the N, O atoms of **pzydmH2** in the equatorial sites [Hg1-O1 = 2.642(3), Hg1-N1 = 2.575(3) Å]. In addition to this, the Hg1 ion is coordinated by the two independent bridging chloride ions in the axial sites [Hg1-Cl1 = 2.3491(9), Hg1-Cl2 = 2.3558(8) Å], thereby forming a see-saw-like coordination environment around Hg1. Therefore, the bite distance of the five-membered chelate ring (Cg(2) = Hg1-O1-C1-C2-N1) is 2.751 Å and gives an angle ∠O1-Hg1-N1 of 63.63(8)° [43]. The Hg2 ion is coordinated by four chloride ions in the equatorial sites, the two terminal chloride ions [Hg2-Cl3 = 2.3182(9), Hg2-Cl4 = 2.3104(8) Å] and the bridging chloride ions [Hg2-$Cl1^i$ = 3.0705(10), Hg2-$Cl2^i$ = 3.0502(10) Å], and the nitrogen atom from **pzydmH2** in the axial position [Hg2-N2 = 2.710(3) Å], to form a distorted square pyramid geometry. The Hg2 ion lies out of the square plane which created

Preprints (www.preprints.org) | NOT PEER-REVIEWED | Posted: 31 May 2023 doi:10.20944/preprints202305.2265.v1



by Cl1$^{i}$, Cl3, Cl2$^{i}$, Cl4 with r.m.s deviation of 0.114 Å. Selected bond lengths, bond and torsion angles of **3** are summarized in Table S2 (see Table S2 for symmetry codes).

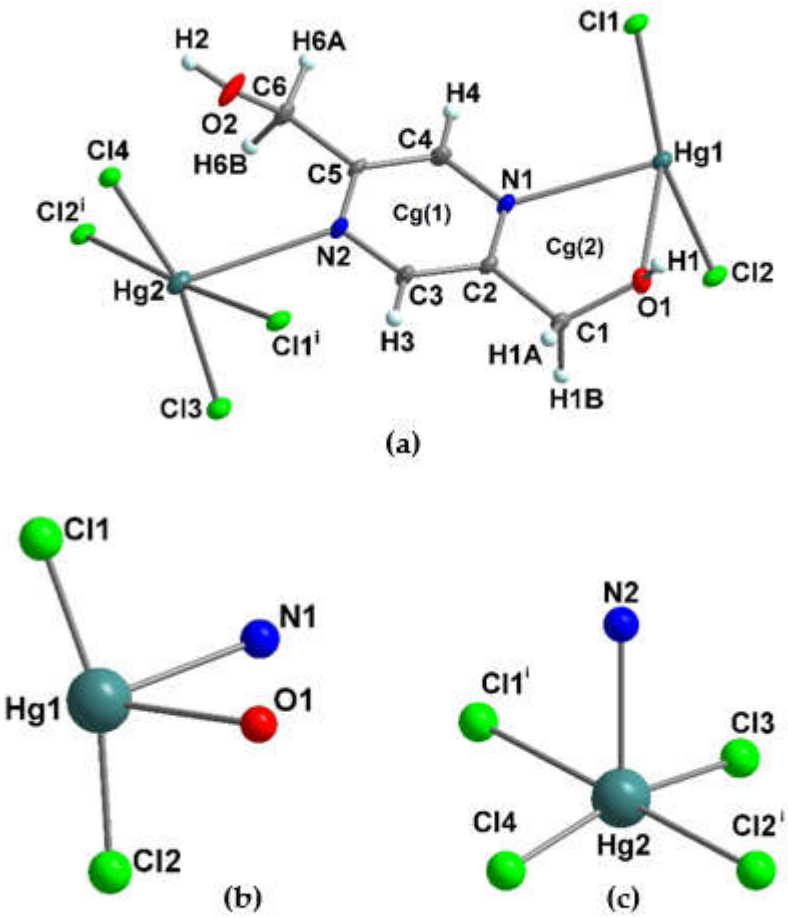


**Figure 9. (a)** Asymmetric unit for **3** along with the atom labelling scheme, the atoms defining the asymmetric unit of the crystal structure **3** are indicated without symmetry codes, displacement ellipsoids at the 50% probability level; H atoms are of arbitrary radii. Symmetry code: i = 2-x,1-y,1-z. Cg(1) = N1-C2-C3-N2-C5-C4, Cg(2) = Hg1-O1-C1-C2-N1. Ball and stick presentations of the coordination environments around **(b)** Hg1 and **(c)** Hg2.

The Hg1 and Hg2 centers are bridged by one **pyzdmH2** (Hg1…Hg2 distance of 8.03(4) Å). Additionally, Hg1 and Hg2 are each connected to adjacent Hg2 and Hg1 centers *via* two pairs of the bridging Cl atoms, with the Cl1-Hg1-Cl2 and Cl1-Hg2-Cl2 angles being 163.73(3)° and 176.69(2)°, respectively. The Hg1…Hg2 distances in these bridging interactions are 3.96(3) Å and 4.01(3) Å. A one-dimensional ladder-like chain was generated through the described connections which extends along the crystallographic *a*-axis (Figure 10). The hydrogen bonds *intra* O1-H1···O2$^{i}$ = **1.93**(2), O1-H1···Cl4$^{i}$ = 2.75(2), C3-H3···Cl1$^{i}$ = 2.81(9), C4-H4···Cl3$^{ii}$ = 2.97(9) and C6-H6B···Cl2$^{ii}$ = 2.95(8) Å respectively from stronger to weaker interaction were identified in each one-dimensional ladder-like chain (Figure 11a and Table S11). Each polymer chain contains symmetrically arranged aromatic pyrazine rings (Cg(1)) that pack almost parallel (alpha ~ 0°) and with a small degree of slippage (slippage ~ 1.5 °) as shown in Figure 11b. The distance between the centroids of the pyrazine rings is relatively long and reported in Table S12. The one-dimensional chains are joined together in a side-to-side fashion by hydrogen bonds between the uncoordinated OH group of **pyzdmH2** in one chain and the oxygen atom from the coordinated OH group of **pyzdmH2** and the chloride atom (Cl2) in a

Preprints (www.preprints.org) | NOT PEER-REVIEWED | Posted: 31 May 2023 doi:10.20944/preprints202305.2265.v1



symmetry-related adjacent chain [O2-H2···O1$^{iii}$ = 2.25(3) Å and O2-H2···Cl2$^{iii}$ = 2.82(4) Å] (Table 1). This creates a 2D sheet that extends within the *ac* plane (Figure 11a, d). Stacking of these sheets along the *b* direction through hydrogen bonds of the C-H···Cl type with range distances between 2.95-3.12 Å yields a 3D non-covalent structure (Figure S7, Table S11). Detailed analysis of the crystal structure revealed *intra-* and *inter* chain Hg···Cl and short halogen bond interactions listed in Table S11 and S13.

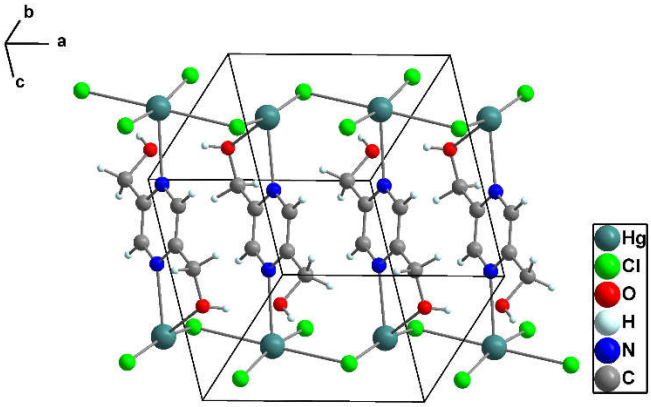


**Figure 10.** One-dimensional ladder-like chain structure along the *a*-axis in the unit cell.

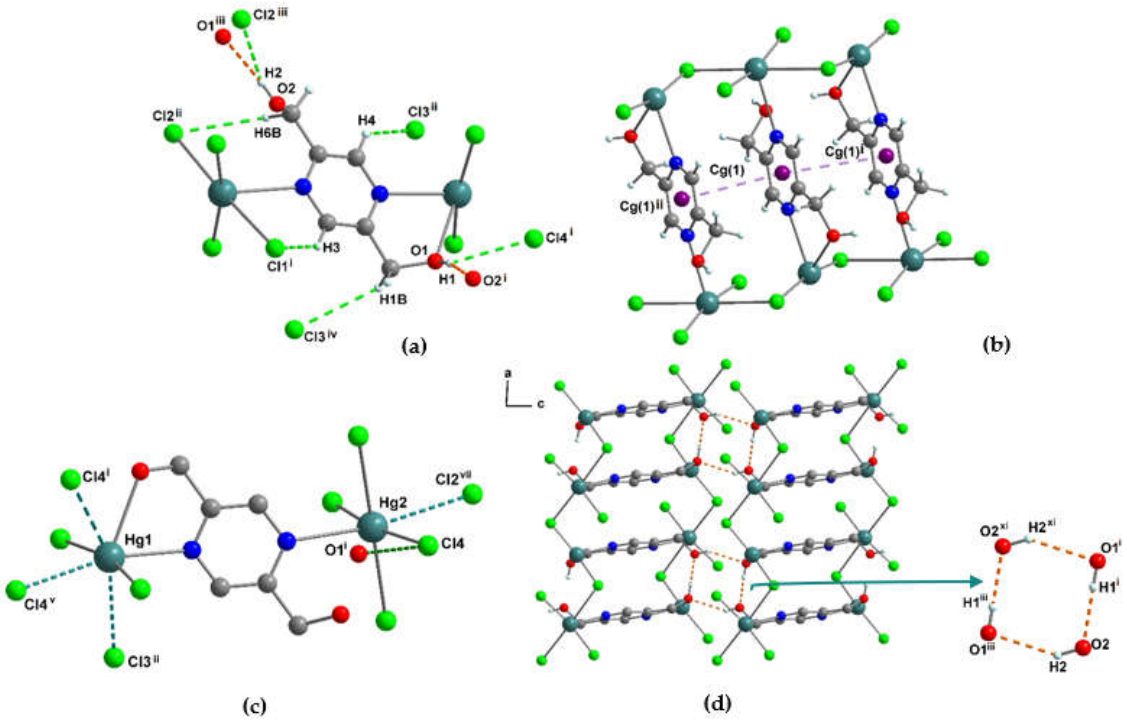


**Figure 11. (a)** Hydrogen bonds of the O-H···O, O-H···Cl and C-H···Cl types are depicted by dashed bonds in orange and light green colors respectively **(b)** π-π (pyrazine ring) interactions are depicted by dashed bonds in light purple color. **(c)** *intra-* and *inter*-chain Hg···Cl, and halogen bond O Cl interactions are depicted by blue-green, and emerald-green colors respectively **(d)** 2D sheet created by the hydrogen bonds of the O-H···O and O-H···Cl types in the *ac* plane along with the magnified depiction of the arrangement of hydrogen bonds of the OH···O type between two one-dimensional ladder-like chains (4-membered cooperative O-H···O-H···O-H···O-H ring). For the sake of clarity, the hydrogens involved in the hydrogen bonds are shown. Symmetry codes i = -x+2, -y+1, -z+1, ii = -x+1, -y+1, -z+1, iii = x, y, z-1, iv = -x+1, -y+2, -z+1, v = x, y-1, z+1, vii = x, y+1, z-1, xi= 2-x, 1-y, -z.

Preprints (www.preprints.org) | NOT PEER-REVIEWED | Posted: 31 May 2023 doi:10.20944/preprints202305.2265.v1



3.1.5. Crystal structure of {[$Cd_2$(pzydm$H_2$)(μ-Cl)$_4$]·$H_2O$}$_n$ (4)

Compound **4** crystallizes in the monoclinic centrosymmetric *C*2/*c* space group (Table S1). **4** is a 3D-neutral coordination polymer in which the $Cd^{2+}$ ion has one type of coordination geometry, a distorted octahedral geometry. As displayed in Figure 12a, the asymmetric unit of the polymeric crystal structure contains one cadmium ion ($Cd^{2+}$), half of pzydmH2 which forms a bridging tetra-dentate characteristic linker, two chloride ions which are coordinated to the cadmium ion in bridging fashion (Cl1 and Cl2), and a non-coordinated crystal water molecule (O2H2AH2B) near a special position (Z = 4, Z' = 0.5). The positive charge on the $Cd^{2+}$ ion is balanced by the two bridging chloride ions.

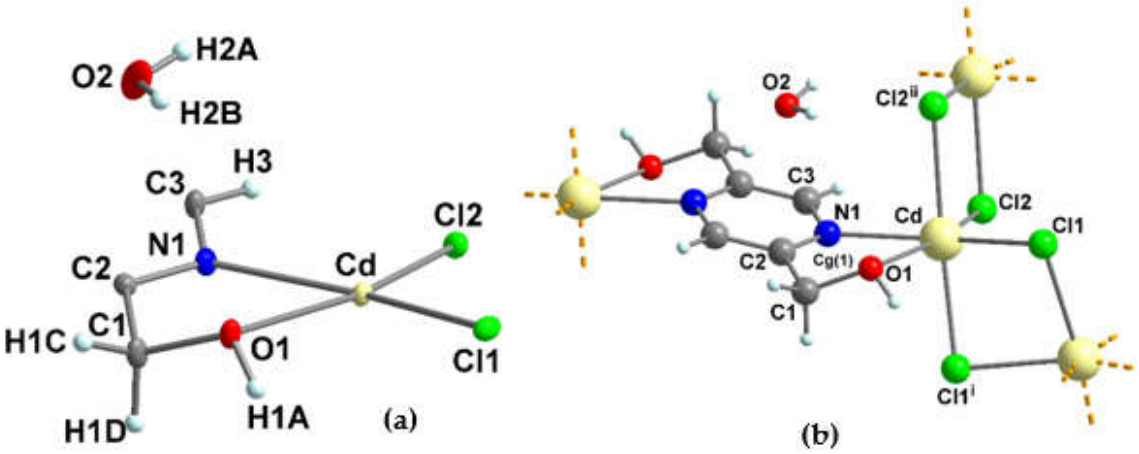


**Figure 12. (a)** Asymmetric unit of **4** along with the atom labelling scheme. For the sake of clarity, hydrogen bonds are omitted. Displacement ellipsoid are draw at the 50% probability level and H atoms are of arbitrary radii. **(b)** Ball and stick presentation of the full coordination environment around the $Cd^{2+}$ in **4**. Symmetry codes: i = 1-x, y, 1/2-z, ii = 1-x, 1-y, 1-z. (Cg(1) = Cd-O1-C1-C2-N1).

As displayed in Figure 12b, the $Cd^{2+}$ ion is in a distorted octahedral coordination geometry by the four bridging chloride ions [Cd–Cl1 = 2.5719(11), Cd–Cl2 = 2.5581(12), Cd-Cl1$^{i}$ = 2.6055(12), Cd-Cl2$^{ii}$ = 2.6752(12) Å] and the oxygen and nitrogen atoms from **pzydmH2** [Cd-O1 = 2.416(3), Cd-N1 = 2.367(4) Å]. The chelating N and O atoms from **pzydmH2** (N1 and O1) are *trans* to the chloride ions Cl1 and Cl2, respectively, and the ∠N1–Cd–O1 and ∠Cl2-Cd-Cl1 bond angles are 69.36(13) and 109.07 (4)° respectively. The N1···O1 bite distance in the five-membered chelate ring is 2.723 Å [43]. The torsion angle ∠O1–C1–C2–N1 in the chelate ring is -36.9(5)° (Figure 12b). The angle between the *trans*-positioned chloride ions, ∠Cl1$^{i}$-Cd-Cl2$^{ii}$ is 173.47(4)°. The bridging chloride ions have slightly different bond distances to the Cd ions, with Cd-Cl1, Cd-Cl2 being shorter than Cd-Cl1$^{i}$, Cd-Cl2$^{ii}$. The shorter Cd-Cl1 and Cd-Cl2 distances can be rationalized on the basis of their *trans*-position to the N and O donors and the resulting *trans*-influence: The stronger π-donating chloride ligands *trans* to the weaker π-donating N and O atoms can form shorter Cd-Cl bonds than the two *trans*-positioned chloride ligands competing for the same d-orbital for π-donation. Table S2 lists the selected bond lengths, bond and torsion angles in **4**.

Each $Cd^{2+}$ center is connected to three neighboring $Cd^{2+}$ centers through the four bridging chloride ions (Cl1, Cl1$^{i}$, Cl2, Cl2$^{ii}$) and one bridging tetra-dentate organic linker **pzydmH2**. The Cd···Cd separations through Cl1, Cl2 and **pzydmH2** are 3.69(6), 3.84(5), 7.46(7) Å respectively. The $Cd^{2+}$ ion connection through the four bridging chloride ions Cl1, Cl1$^{i}$, Cl2, and Cl2$^{ii}$ constructs a crenellation-like chain along the crystallographic *c*-axis (Figure 13a). The chain consists of two types of four-membered rings with square planes, where the dihedral angle between adjacent rings is 82.9° and the bond angles ∠Cd-Cl1-Cd$^{i}$ and ∠Cd-Cl2-Cd$^{ii}$ are 90.96(4) and 94.51(4)° respectively (Figure 13b). These two types of four-membered rings alternately repeat along the crystallographic *c*-axis to construct the crenellation-like chain (Figure 13a). It is appropriate to mention that the distortion from the octahedral geometry around $Cd^{2+}$ is due to the angle strain present in the four-membered ring Cg(3) and the constraint imposed by the chelation on the bond angle ∠N1–Cd–O1. Each crenellation-

Preprints (www.preprints.org) | NOT PEER-REVIEWED | Posted: 31 May 2023 doi:10.20944/preprints202305.2265.v1



like chain connects to the four neighboring crenellation-like chains through the **pzydmH2** linkers so that a 3D coordination network is been generated (Figure 13c, d). The 3D network accommodates the crystal water molecules by the four hydrogen bonds O2-H2B···O1$^{iv}$ = 1.85, O1-H1A···O2$^{x}$ = 1.83(10), O2-H2A···Cl2$^{ii}$ = 2.65(13), and O2-H2A···Cl2$^{v}$ = 2.68(13) Å (Figure 14b, Figure 15a, Table 1 and Table S14), by which an infinite hydrogen-bond chain O-H···O-H···O-H·· is formed between the two crenellation-like chains in **4** (Figure 15d). Figure S8a depicts the asymmetric unit where H1B is attached to the oxygen atom from **pzydmH2**.

Upon conducting a comprehensive analysis of the crystal structure through the PLATON full geometry calculation [multiple hydrogen bond and halogen bond interactions were identified and are presented in Figure 15 and listed in Table S14 and Table S15. Table 1 lists the strongest hydrogen-bond interactions found in the crystal structure [45–50].

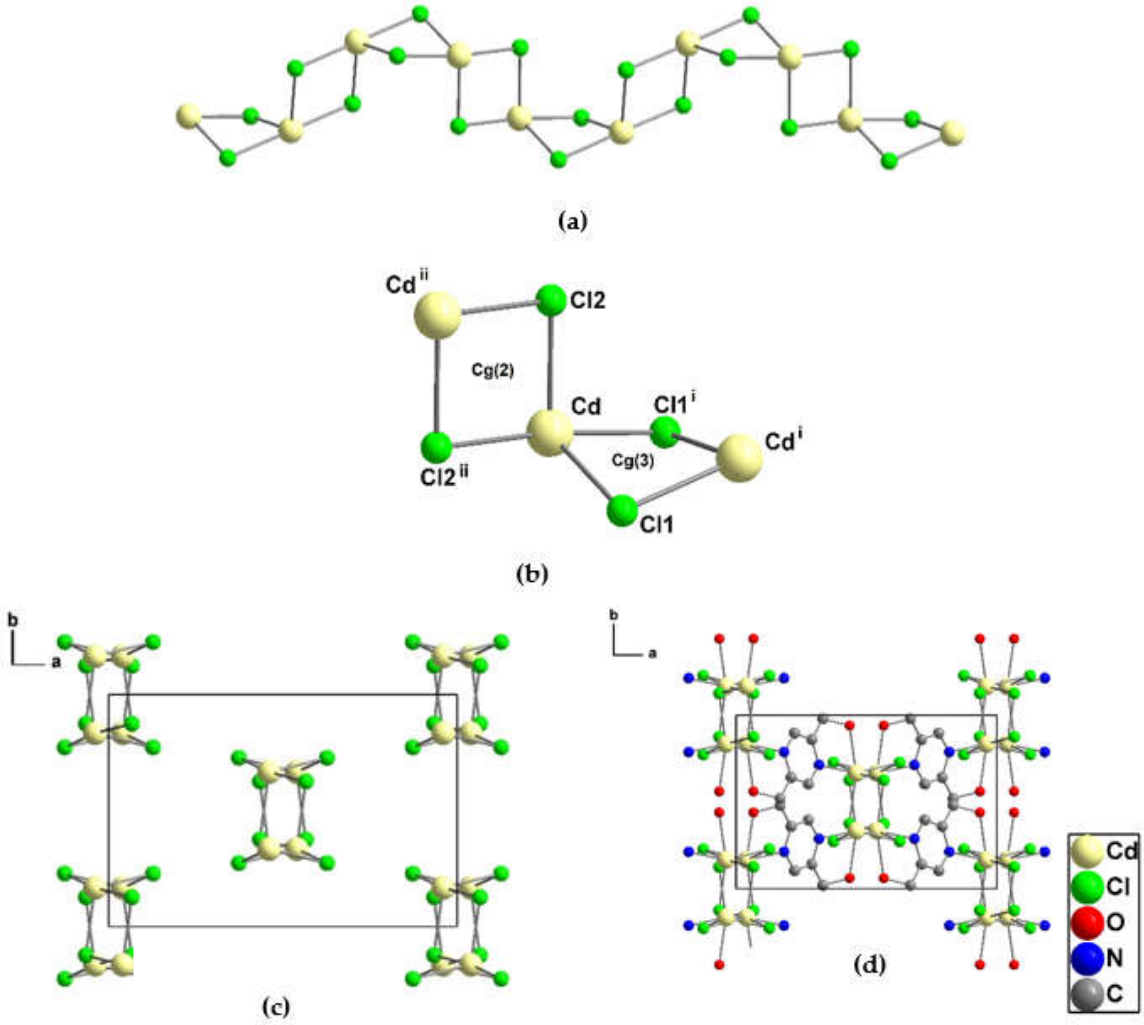


**Figure 13. (a)** One-dimensional crenellation-like chain structure constructed from Cd and Cl atoms in **4**. **(b)** Two alternating square-like rings Cg(2) and Cg(3), ((Cg(2) = Cd, Cl2, Cd$^{ii}$, Cl2$^{ii}$ with r.m.s deviation of 0.000 Å and Cg(3) = Cd, Cl1, Cd$^{i}$, Cl1$^{i}$ with r.m.s deviation of 0.265 Å). **(c)** Ball and stick presentation of the five crenellation-like chains and **(d)** the unit cell of **4** viewed along the *c*-axis. Hydrogen atoms and crystal water molecules omitted for the sake of clarity. Symmetry codes: i = -x+1, y, -z+1/2, ii = -x+1, -y+1, -z+1.

Preprints (www.preprints.org) | NOT PEER-REVIEWED | Posted: 31 May 2023 doi:10.20944/preprints202305.2265.v1



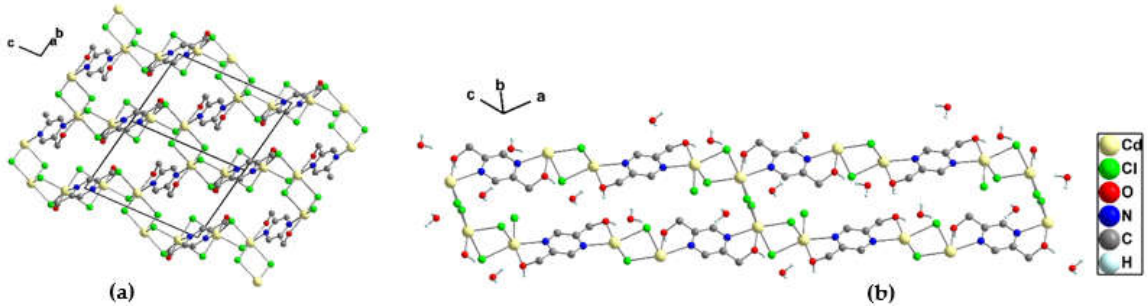


**Figure 14. (a)** The unit cell packing within the *bc* plane. For the sake of clarify, H atoms and the crystal water molecules were omitted. **(b)** Simplified view of the empty space along with the crystal water molecules in **4**. For the sake of clarify, H atoms from the crystal water molecules and hydroxyl groups are only depicted.

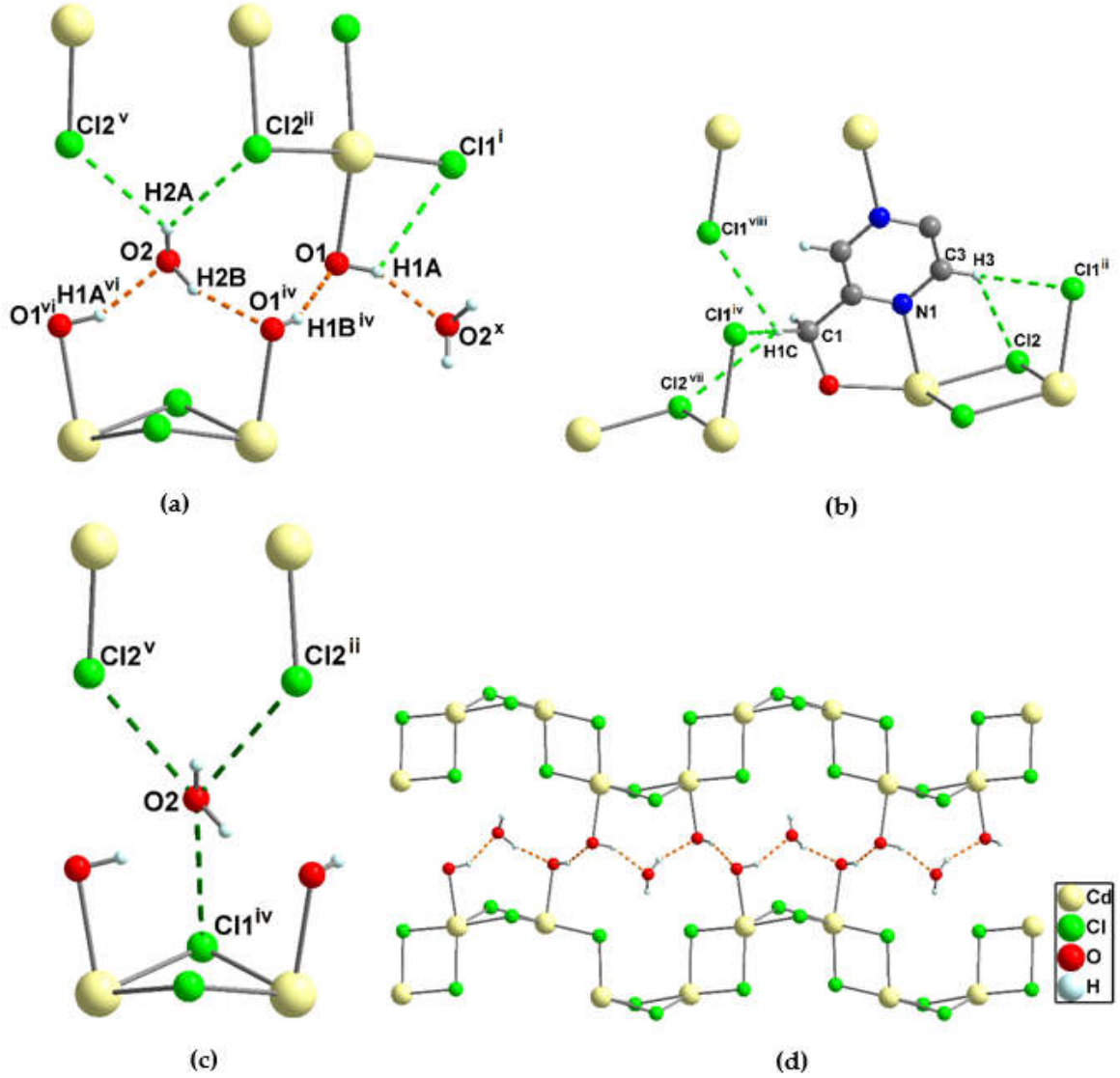


**Figure 15. (a)** Hydrogen bonds of the O-H···O and O-H···Cl types are depicted by dashed bonds in orange and light green colors respectively. **(b)** Hydrogen bonds of the C-H···Cl type and **(c)** halogen bond interactions are depicted by dashed bonds in light and dark green colors respectively. **(d)** Zig-zag arrangement of crystal water molecules in **4**. Symmetry codes: i = 1-x, y, 1/2-z, ii = -x+1, -y+1, -z+1,

Preprints (www.preprints.org) | NOT PEER-REVIEWED | Posted: 31 May 2023 doi:10.20944/preprints202305.2265.v1



iii = -x+1/2, -y+1/2, -z+1, iv = -x+1, -y, -z+1, v = x, 1-y, 1/2+z, vi = x, -y, 1/2+z, vii = x, -1+y, z, viii = x-1/2, y-1/2, z, x = x, -y, -1/2+z.

3.1.6. Crystal structure of $\{[Cd_2(pzydmH2)(\mu\text{-}Br)_4].H_2O\}_n$ (5)

The results of single-crystal X-ray diffraction analysis revealed that compound **5** has an isostructural relationship to compound **4**. Both compounds share the same space group (monoclinic centrosymmetric *C*2/*c*) and have similar atomic arrangements, but their chemical compositions differ due to the replacement of Cl in compound **4** with Br in compound **5**. Although the crystallographic parameters of the two structures are not identical, they exhibit a high degree of similarity (Table S1). The unit cell parameters of **5** are within 3.6% of those of **4**, with the lattice constants a, b, and c being 14.12, 9.00 Å, and 12.02 Å, respectively, compared to 14.02, 8.69, and 11.70 Å in **4**. The value of Beta angle in **5** is 109.6(3)° compared to 111.1(2)° in **4**. The asymmetric unit in **5** contains, one independent cadmium ion ($Cd^{2+}$) with a distorted octahedral coordination geometry, half of **pzydmH2** which forms a bridging tetra-dentate characteristic linker, two bromine ions which are coordinated to the cadmium ion in the bridging fashion (Br1 and Br2), all atoms are in general positions, and finally a non-coordinated water molecule (O2H2AH2B) near a special position (Z = 4, Z' = 0.5). Figure 16a and b show the asymmetric unit and the full coordination environment around the Cd ion.

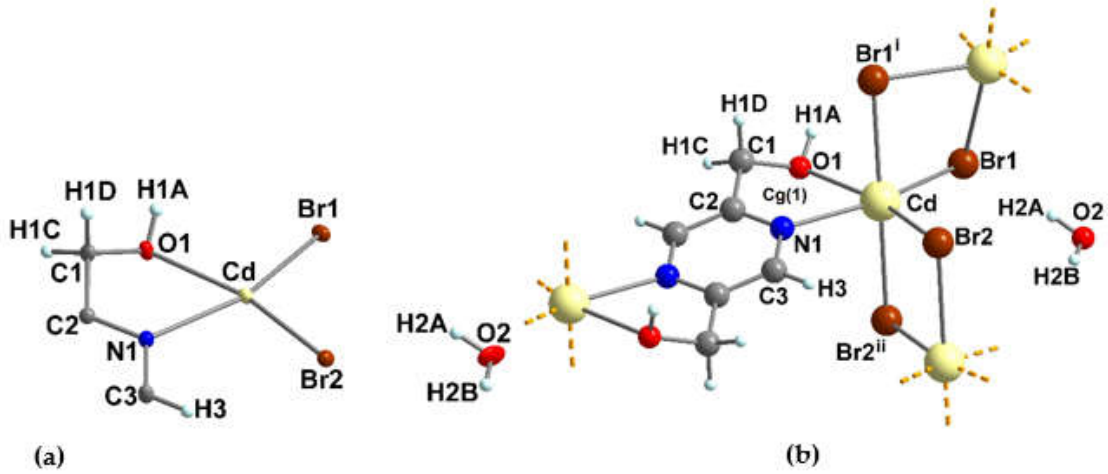


**Figure 16. (a)** Asymmetric unit of the crystal structure **5** along with the atom labelling scheme. For the sake of clarity, hydrogen bonds are omitted. Displacement ellipsoids are drawn at the 50% probability level and H atoms are of arbitrary radii. **(b)** Ball and stick presentation of the full coordination environment around $Cd^{2+}$ in **5**. Symmetry codes: i = 1-x, y, -z+3/2 and ii = 1-x, 1-y, 1-z.

**5** has a similar coordination geometry around the $Cd^{2+}$ ion as the derivative Cl compound. The $Cd^{2+}$ ion is coordinated by the four bridging bromine ions and the nitrogen and oxygen atoms from **pzydmH2** so that the bite distance in the five-membered chelate ring (Cg(1) = Cd-O1-C1-C2-N1) is 2.74 Å. The equatorial plane is occupied by the chelating N and O atoms from **pzydmH2** and the two bridging bromides (Br1, Br2) and the axial positions are occupied by the two symmetry-related bridging bromides ($Br1^{i}$, $Br2^{ii}$). The selected bond lengths, angles, and torsion angles for **4** and **5** can be compared in Table S2. (See Table S1 for symmetry codes).

The 3D structure of **5** is analogous to **4**, where $Cd^{2+}$ centers are linked to neighboring $Cd^{2+}$ centers *via* the bridging bromide ions (Br1, $Br1^{i}$, Br2, $Br2^{ii}$) resulting in a crenellation-like chain structure along the crystallographic *c*-axis (Figure S8a, b) and the bridging tetra-dentate organic linker **pzydmH2** (Figure S8c, d). In the 3D structure, Cd···Cd separations by the bridging bromide ions and **pzydmH2** are 3.7981(6) Å, 3.9635(5) Å, and 7.4928(7) Å respectively. As depicted in Figure 17a the water molecules in the 3D coordination network are accommodated by the hydrogen bond interactions involving O1-H1A$^{vi}$···O2, O2-H2B···O1$^{v}$, O2-H2B···Br2 and O2-H2B···$Br2^{i}$ (Figure S9a, b) [51]. Like structure **4**, structure **5** also has infinite chains of O-H···O-H···O-H···, which result from the hydrogen

Preprints (www.preprints.org) | NOT PEER-REVIEWED | Posted: 31 May 2023 doi:10.20944/preprints202305.2265.v1



bond interactions between the hydroxyl groups of **pzydmH2** and crystal water molecules in **5**. The hydrogen bond distances are listed in Table 1. Figure 17b shows the arrangement of the crystal water molecules between two crenellation-like chains in **5**. Several non-covalent interactions involving hydrogen bonds and halogen bonds have been identified in **5** listed in Tables S16 and S17.

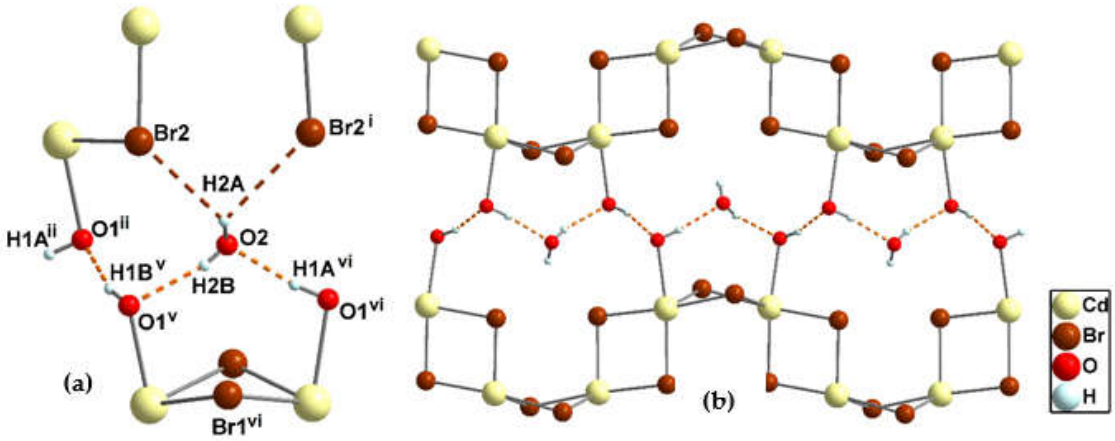


**Figure 17. (a)** Hydrogen bonds of the O-H···O, and O-H···Br types are depicted by dashed bonds in orange color and brick red color respectively. **(b)** Zig-zag arrangement of crystal water molecules in **5**. Symmetry codes: i = -x+1, y, -z+3/2, ii = -x+1, -y+1, -z+1, v = x, y+1, z, vi = 1-x, y+1, 3/2-z.

*3.3. IR studies*

Based on the comparison of IR spectra of **pzydmH2**, **2**, **3**, and **5**, certain vibrations were identified. These vibrations correspond to the perturbations of O-$H_{alcohol}$ and O-$H_{crystal\ water}$ due to the strong hydrogen bond interactions. In **2**, the vibrations of O-$H_{alcohol}$ and O-$H_{crystal\ water}$ perturbed by the strong hydrogen bond interactions were identified as 3408, 3340, 3269, and 3183 $cm^{-1}$. In **3**, the vibrations of O-$H_{alcohol}$ perturbed by the hydrogen bond interactions were identified as 3486 and 3275 $cm^{-1}$, and there were no vibrations of O-$H_{crystal\ water}$ as expected. In **5**, the vibrations of O-$H_{alcohol}$ perturbed by the hydrogen bond interactions were identified as 3546 and 3419 $cm^{-1}$, while the vibrations of O-$H_{crystal\ water}$ perturbed by the hydrogen bonds were identified as 3108 and 1587 $cm^{-1}$. The vibrations of C-$H_{aromatic}$ and C-$H_{aliphatic}$ involved in the formation of the hydrogen bonds were identified as 3033, 2827, and 2808 $cm^{-1}$ (refer to Figure S10-13) [52]. The IR and CNH analyses confirmed the presence of crystal water molecules in **2** and **5**, as well as the strong hydrogen bond interactions observed in the single crystal structures of **2**, **3**, and **5**.

## 4. Conclusion

In this paper, we reported the synthesis and crystal structures of pyrazine diyldimethanol (**pzydmH2**) and three 1D (**1**-**3**) and two isostructural 3D coordination compounds (**4**, **5**). **1**-**5** assembled from **pzydmH2** with the metal halide salts of $CuBr_2$, $ZnCl_2$, $HgCl_2$, $CdCl_2{\cdot}H_2O$ and $CdBr_2{\cdot}4H_2O$ in water under ambient conditions respectively. With the exception of compound **3**, **1**-**5** each contained crystal water molecules within their structures. **PzydmH2**, which acts as a bridging tetra-dentate linker with N,O-chelating capability in the reported structures **1**-**5** (tri-dentate in **3**), is weakly acidic. The OH groups in the methanol parts have not intended to be de-pronate and have provided a moiety for forming strong hydrogen bond interactions. The 1D and 3D coordination compounds featured the strong hydrogen bonds between the hydroxyl groups from the organic ligand, coordinated and non-coordinated water molecules in the structures including the OH···O type hydrogen bond interaction in which the hydroxyl group as a donor and oxygen atom as an acceptor with the bond distance ranges 1.72-2.87 Å, the OH···X (X = N, Cl, Br) type hydrogen bond interaction in which the hydroxyl group as a donor and nitrogen or halogen atoms as an acceptor with the bond distance ranges 1.97-3.21 Å as well as the C-$H_{aromatic}$/C-$H_{aliphatic}$···X (X = O, Cl, Br) type hydrogen bond

interactions in which the C-$H_{aromatic}$ and C-$H_{aliphatic}$ groups as donors and the oxygen or halogen atom as an acceptor with the bond distance ranges 2.42-3.24 Å. The short halogen bond interaction of the donor halogens (Br, Cl) with the electronegative heteroatom (O) with the bond distance ranges 3.08-3.48 Å have been found in **1**-**5**. The results showed that the both bridged **pzydmH2** and halogen ions as well as the hydrogen bond interactions involved with the hydroxyl groups from **pzydmH2** and water molecules play the most important roles in the 3D non-covalent and covalent structure construction in **1**-**5**. Given the high water solubility and versatility of **pzydmH2** as a bridging tetra-dentate organic linker with the ability N,O-chelating capable of engaging in various non-covalent interactions as seen in the newly synthesized compounds, we are motivated to synthesize and investigate other ligand derivatives with elongated or angled skeletons for fabricating porous coordination compounds. Such compounds can be synthesized without using hazardous organic solvents, elevated temperature or pressure, and have potential applications in reversible adsorption of small molecules or biologically relevant molecules, owing to the presence of hydroxyl groups, hydrophilic pores, voids or empty spaces, and ability to form robust hydrogen bonding networks. This presents an exciting research direction that has been long sought after.

**Supplementary Materials:** CCDC numbers 2232274, 2232622, 2253333, 2236315, 2249852, and 2236379 for **pzdmH2** and **1-5** respectively. $^{1}H$ and $^{13}C$ NMR spectra for dimethyl pyrazine-2,5-dicarboxylate and **pzdmH2**. Crystallographic data including structure determination and refinement details as well as selected bond lengths, angles and torsion angles for **pzydmH2** and **1–5**. Tables listing the data for short non-covalent interactions for **pzydmH2** and **1–5**. Reciprocal lattice plot of the non-merohedral twin crystal **2**. Crystal packing diagram of **pzydmH2, 3** and **5**. IR spectra of **2**, **3**, and **5**.

**Funding:** Funding for this research was provided by German Research Foundation DFG (Grant number 1460232).

**Acknowledgements:** We express our gratitude to the German Research Foundation (DFG) for their financial support of this study.

**Conflicts of Interest:** The authors declare no conflict of interest.

## References

1. Armaghan M, Niu RJ, Liu Y, Zhang WH, Hor TA, Lang JP. Zn-based metal–organic frameworks (MOFs) of pyridinemethanol–carboxylate conjugated ligands: Deprotonation-dependent structures and $CO_2$ adsorption. *Polyhedron*. **2018**, 153, 218-25. [https://doi.org/10.1016/j.poly.2018.07.029]
2. Armaghan M, Lu WJ, Wu D, Wei Y, Yuan FL, Ng SW, Amini MM, Zhang WH, Young DJ, Hor TA, Lang JP. Isolation of first row transition metal-carboxylate zwitterions. *RSC Adv.* **2015**, 5, 42978-89. [10.1039/C5RA05564D]
3. Armaghan M, Shang XJ, Yuan YQ, Young DJ, Zhang WH, Hor TA, Lang JP. Metal–Organic Frameworks via Emissive Metal-Carboxylate Zwitterion Intermediates. *ChemPlusChem.* **2015**, 80, 1231-4. [https://doi.org/10.1002/cplu.201500134]
4. Ma PP, Hao ZM, Wang P, Zhang WH, Young DJ. trans-$[Ni(pdm)_2]^{2+}$(pdm= 2-pyridinemethanol) as a reliable synthon for isoreticular metal–organic frameworks of linear dicarboxylates. *J. Solid State Chem.* **2023**, 317, 123721. [https://doi.org/10.1016/j.jssc.2022.123721]
5. Liu Y, Lin SX, Niu RJ, Liu Q, Zhang WH, Young DJ. Zinc and cadmium complexes of pyridinemethanol carboxylates: Metal carboxylate zwitterions and metal–organic frameworks. *ChemPlusChem*. **2020**, 85, 832-7. [https://doi.org/10.1002/cplu.202000175]
6. Telfer SG, Kuroda R, Lefebvre J, Leznoff DB. Boxes, helicates, and coordination polymers: A structural and magnetochemical investigation of the diverse coordination chemistry of simple pyridine-alcohol ligands. *Inorg. chem.* **2006**, 45, 4592-601. [https://doi.org/10.1021/ic0517218]
7. Taguchi T, Stamatatos TC, Abboud KA, Jones CM, Poole KM, O'Brien TA, Christou G. New Fe4, Fe6, and Fe8 clusters of iron (III) from the use of 2-pyridyl alcohols: structural, magnetic, and computational characterization. *Inorg. chem*. **2008**, 47, 4095-108. [https://doi.org/10.1021/ic701756p]
8. Telfer SG, Sato T, Kuroda R. Noncovalent Ligand Strands for Transition-Metal Helicates: The Straightforward and Stereoselective Self-Assembly of Dinuclear Double-Stranded Helicates Using Hydrogen Bonding. *Angew. Chem. Int. Ed.* **2004**, 43, 581-4. [https://doi.org/10.1002/anie.200352833]
9. Olguín J, Brooker S. Spin crossover active iron (II) complexes of selected pyrazole-pyridine/pyrazine ligands. *Coord. Chem. Rev.* **2011**, 255, 203-40. [https://doi.org/10.1016/j.ccr.2010.08.002]
10. Wang JF, Feng T, Li YJ, Sun YX, Dong WK, Ding YJ. Novel structurally characterized Co (II) metal-organic framework and Cd (II) coordination polymer self-assembled from a pyridine-terminal salamo-like ligand

bearing various coordination modes. *J. Mol. Struct.* **2021**,1231, 129950. [https://doi.org/10.1016/j.molstruc.2021.129950]
11. Telfer SG, Kuroda R. The Versatile, Efficient, and Stereoselective Self-Assembly of Transition-Metal Helicates by Using Hydrogen-Bonds. *Chem. Eur. J.* **2005**,11, 57-68. [https://doi.org/10.1002/chem.200400485]
12. Zhang J, Teo P, Pattacini R, Kermagoret A, Welter R, Rogez G, Hor TA, Braunstein P. Structural Effects of Sodium Cations in Polynuclear, Multicubane-Type Mixed Na–Ni Complexes. *Angew. Chem.* **2010**, 122, 4545-8. [https://doi.org/10.1002/ange.201001412]
13. Stamatatos TC, Abboud KA, Wernsdorfer W, Christou G. High-Nuclearity, High-Symmetry, High-Spin Molecules: A Mixed-Valence Mn10 Cage Possessing Rare T symmetry and an S=22 Ground State. *Angew. Chem.* **2006**, 118, 4240-3. [https://doi.org/10.1002/ange.200600691]
14. Ramírez J, Brelot L, Osinska I, Stadler AM. CH…O hydrogen bond in the crystal structure of a pyrazine-based ligand and determination of the amplitude of the ligand conformational change induced by Cu (II) coordination. *J. Mol. Struct.* **2009**, 931, 20-4. [https://doi.org/10.1016/j.molstruc.2009.05.021]
15. Ferreira SB, Kaiser CR. Pyrazine derivatives: a patent review (2008–present). *Expert Opin. Ther. Patents.* **2012**, 22,1033-51. [https://doi.org/10.1517/13543776.2012.714370]
16. Juhas M, Zitko J. Molecular interactions of pyrazine-based compounds to proteins. *J. Med. Chem.* **2020**, 63, 8901-16. [https://doi.org/10.1021/acs.jmedchem.9b02021]
17. Riel AM, Rowe RK, Ho EN, Carlsson AC, Rappé AK, Berryman OB, Ho PS. Hydrogen bond enhanced halogen bonds: a synergistic interaction in chemistry and biochemistry. *Acc. Chem. Res.* **2019**, 52, 2870-80. [https://doi.org/10.1021/acs.accounts.9b00189]
18. Azbell TJ, Pitt TA, Bollmeyer MM, Cong C, Lancaster KM, Milner P. Ionothermal Synthesis of Metal-Organic Frameworks Using Low-Melting Metal Salt Precursors. *Angew. Chem.* **2023**, 135, e202218. [https://doi.org/10.26434/chemrxiv-2022-00xd7]
19. Guerah NE, Zerrouki K, Benslama O, Daran JC, Bouacida S, Bouchene R. New polymorph for Cd (II) chloro-bridged coordination polymer based on 3-aminopyrazin-2-carboxylic acid: Synthesis, structural characterization, Hirshfeld surface analysis, thermal properties and molecular docking study on the antifungal activity. *J. Mol. Struct.* **2022**, 1258, 132681. [https://doi.org/10.1016/j.molstruc.2022.132681]
20. Bruker AXS, APEX2, Bruker AXS Inc., Madison, Wisconsin, USA, 2012.
21. APEX4 v2021.4-1, 2003, 2004 Bruker Nonius.
22. APEX4 v2021.4-1, 2005-2018 Bruker AXS.
23. APEX4 v2021.4-1, 2019, 2020 Bruker Nano.
24. APEX4 v2021.4-1, 2021 Bruker AXS.
25. SMART, data collection program for the CCD Area-Detector System; SAINT, data reduction and frame integration program for the CCD area-detector system. Bruker analytical X-ray systems, Madison, Wisconsin, USA, 1997.
26. G. M. Sheldrick, in Program SADABS: Area-detector absorption correction, University of Göttingen, Germany, 1996.
27. Sheldrick GM. SHELXT–Integrated space-group and crystal-structure determination. *Acta Cryst.* **2015**, A71, 3-8. [https://doi.org/10.1107/S2053273314026370]
28. Sheldrick GM. Crystal structure refinement with SHELXL. *Acta Cryst.* **2015**, C71, 3-8. [https://doi.org/10.1107/S2053229614024218]
29. Dolomanov OV, Bourhis LJ, Gildea RJ, Howard JA, Puschmann H. OLEX2: a complete structure solution, refinement and analysis program. *J. appl. cryst.* **2009**, 42, 339-41. [https://doi.org/10.1107/S0021889808042726]
30. Hübschle CB, Sheldrick GM, Dittrich B. ShelXle: a Qt graphical user interface for SHELXL. *J. appl. cryst.* **2011**, 44, 1281-4. [https://doi.org/10.1107/S0021889811043202]
31. K. Brandenburg, DIAMOND (Version 4.6.8), Crystal and Molecular Structure Visualization, Crystal Impact, Dr. H. Putz & Dr. K. Brandenburg GbR, Bonn Germany, 1997–2022, http://www.crystalimpact.com/diamond.
32. Macrae CF, Sovago I, Cottrell SJ, Galek PT, McCabe P, Pidcock E, Platings M, Shields GP, Stevens JS, Towler M, Wood PA. Mercury 4.0: From visualization to analysis, design and prediction. *J. appl. cryst.* **2020**, 53, 226-35. [https://doi.org/10.1107/S1600576719014092]
33. Macrae CF, Bruno IJ, Chisholm JA, Edgington PR, McCabe P, Pidcock E, Rodriguez-Monge L, Taylor R, Streek JV, Wood PA. Mercury CSD 2.0–new features for the visualization and investigation of crystal structures. *J. Appl. Cryst.* **2008**, 41, 466-70. [https://doi.org/10.1107/S0021889807067908]
34. Macrae CF, Edgington PR, McCabe P, Pidcock E, Shields GP, Taylor R, Towler M, Streek JV. Mercury: visualization and analysis of crystal structures. Journal of applied crystallography. 2006, 39, 453-7.
35. Steiner T. The hydrogen bond in the solid state. *Angew. Chem. Int. Ed.* **2002**, 41, 48-76. [https://onlinelibrary.wiley.com/doi/10.1002/1521-3773(20020104)41:1%3C48::AID-ANIE48%3E3.0.CO;2-U]

36. Riel AM, Rowe RK, Ho EN, Carlsson AC, Rappé AK, Berryman OB, Ho PS. Hydrogen bond enhanced halogen bonds: a synergistic interaction in chemistry and biochemistry. *Acc. Chem. Res*. **2019**, 52, 2870-80. [https://doi.org/10.1021/acs.accounts.9b00189]
37. Prasanna MD, Row TG. C–halogen···π interactions and their influence on molecular conformation and crystal packing: A database study. *Cryst. eng*. **2000**, 3, 135-54. [https://doi.org/10.1016/S1463-0184(00)00035-6]
38. Dolai G, Roy S, Sen S, Giri RS, Mandal B. Crystal structure of 1-(2, 4, 6-trichlorobenzoyloxy) benzotriazole (TCB-OBt): observation of uncommon intermolecular oxygen–oxygen interaction and synthetic application in amidation. *New J. Chem*. **2021**, 45, 19804-11. [10.1039/D1NJ04048K]
39. Groizard T, Kahlal S, Dorcet V, Roisnel T, Bruneau C, Halet JF, Gramage-Doria R. Nonconventional Supramolecular Self-Assemblies of Zinc (II)–Salphen Building Blocks. *Eur. J. Inorg. Chem*. **2016**, 32, 5143-51. [https://doi.org/10.1002/ejic.201600866]
40. Sharma C, Singh AK, Joy J, Jemmis ED, Awasthi SK. Experimental and theoretical study of intramolecular O···O interaction in structurally rigid β-keto carboxylic esters. *RSC adv*. **2016**, 6, 91689-93. [10.1039/C6RA20483J]
41. Gleiter R, Haberhauer G, Werz DB, Rominger F, Bleiholder C. From noncovalent chalcogen–chalcogen interactions to supramolecular aggregates: experiments and calculations. *Chem. Rev.* **2018**, 118, 2010-4. [https://doi.org/10.1021/acs.chemrev.7b00449]
42. C. Janiak, A critical account on pi-pi stacking in metal complexes with aromatic nitrogen-containing ligands. *J. Chem. Soc., Dalton Trans*. **2000**, 3885-3896. [https://doi.org/10.1039/B003010O]
43. Alvarez S. Distortion pathways of transition metal coordination polyhedra induced by chelating topology. *Chem. Rev.* **2015**, 115, 13447-83. [https://doi.org/10.1021/acs.chemrev.5b00537]
44. Molčanov K, Kojić-Prodić B. Towards understanding π-stacking interactions between non-aromatic rings. *IUCrJ*. **2019**, 6, 156-66. [https://doi.org/10.1107/S2052252519000186]
45. Spek AL. Structure validation in chemical crystallography. *Acta Cryst.* **2009**, D65, 148-55. [https://doi.org/10.1107/S090744490804362X]
46. Spek AL. Single-crystal structure validation with the program PLATON. *J. Appl. Crystallogr.*, **2003**, 36, 7-13. [https://doi.org/10.1107/S0021889802022112]
47. Spek AL. What makes a crystal structure report valid?. *Inorganica Chim. Acta.*, **2018**, 470, 232-7. [https://doi.org/10.1016/j.ica.2017.04.036]
48. Spackman MA, Jayatilaka D. Hirshfeld surface analysis. *CrystEngComm*. **2009**, 11, 19-32. [https://doi.org/10.1039/B818330A]
49. Spackman MA, McKinnon JJ. Fingerprinting intermolecular interactions in molecular crystals. *CrystEngComm*. **2002**, 4, 378-92. [https://doi.org/10.1039/B203191B]
50. Hogue RW, Dhers S, Hellyer RM, Luo J, Hanan GS, Larsen DS, Garden AL, Brooker S. Self-Assembly of Cyclohelicate [M3L3] Triangles Over [M4L4] Squares, Despite Near-Linear Bis-terdentate L and Octahedral M. *Chem. Eur. J*. **2017**; 23, 14193-9. [https://doi.org/10.1002/chem.201702153]
51. Turner MJ, McKinnon JJ, Jayatilaka D, Spackman MA. Visualisation and characterisation of voids in crystalline materials. *CrystEngComm*. **2011**, 13, 1804-13. [https://doi.org/10.1039/C0CE00683A]
52. Nibbering ET, Dreyer J, Kühn O, Bredenbeck J, Hamm P, Elsaesser T. Vibrational dynamics of hydrogen bonds. *Analysis and control of ultrafast photoinduced reactions*. Kühn O, Wöste L, Eds.; Springer series in chemical physics: Germany, **2007**, pp. 619-87.